Joint Ranging and Phase Offset Estimation for Multiple Drones using ADS-B Signatures

Mohammadkarimi, Mostafa; Leus, Geert; Rajan, Raj Thilak

Important note
To cite this publication, please use the final published version (if applicable).
Please check the document version above.

Joint Ranging and Phase Offset Estimation for Multiple Drones Using ADS-B Signatures

Mostafa Mohammadkarimi ⓘ, *Member, IEEE*, Geert Leus ⓘ, *Fellow, IEEE*,
and Raj Thilak Rajan ⓘ, *Senior Member, IEEE*

Abstract—A new method for joint ranging and Phase Offset (PO) estimation of multiple drones/aircrafts is proposed in this paper. The proposed method employs the superimposed unco-ordinated Automatic Dependent Surveillance-Broadcast (ADS-B) packets broadcasted by drones/aircrafts for joint range and PO estimation. It jointly estimates range and PO prior to ADS-B packet decoding; thus, it can improve air safety when packet decoding is infeasible due to packet collision. Moreover, it enables coherent detection of ADS-B packets, which can result in more reliable multiple target tracking in aviation systems using cooperative sensors for detect and avoid (DAA). By minimizing the Kullback-Leibler Divergence (KLD) statistical distance measure, we show that the received complex baseband signal coming from K uncoordinated drones/aircrafts corrupted by Additive White Gaussian Noise (AWGN) at a single antenna receiver can be approximated by an independent and identically distributed (i.i.d.) Gaussian Mixture (GM) with 2^K mixture components in the two-dimensional (2D) plane. While direct joint Maximum Likelihood Estimation (MLE) of range and PO from the derived GM Probability Density Function (PDF) leads to an intractable maximization, our proposed method employs the Expectation-Maximization (EM) algorithm to estimate the modes of the 2D Gaussian mixture followed by a reordering estimation technique through combinatorial optimization to estimate range and PO. An extension to a multiple antenna receiver is also investigated in this article. While the proposed estimator can estimate the range of multiple drones/aircrafts with a single receive antenna, a larger number of drones/aircrafts can be supported with higher accuracy by the use of multiple antennas at the receiver. The effectiveness of the proposed estimator is supported by simulation results. We show that the proposed estimator can jointly estimate the range of multiple drones/aircrafts accurately.

Index Terms—ADS-B, cooperative navigation, detect and avoid (DAA), expectation-maximization (EM), Gaussian mixture (GM), multiple receive antennas, phase offset, range estimation.

I. INTRODUCTION

AUTOMATIC Dependent Surveillance-Broadcast (ADS-B) is one of the two Automatic Dependent Surveillance (ADS) systems that tracks aircrafts without employing radar.

It is intended to improve traffic surveillance capabilities by sharing accurate aircraft position information between pilots and air traffic controllers. In the ADS-B system, aircrafts regularly and asynchronously broadcast their real-time position information, velocity, and identification to no specific receiver using a transponder, typically combined with a Global Positioning System (GPS), to transmit highly accurate positional information to traffic controllers and directly to other aircrafts. This transmission is known as ADS-B Out and its accuracy and update rate are much greater than conventional primary radar surveillance. The reception of the ADS-B packet by an aircraft is ADS-B In [1], [2], [3].

ADS-B system is considered a promising solution to enable safe autonomous drone navigation, especially in urban environments [4]. In order to avoid aviation accidents, each drone needs to be aware of the position and speed of the surrounding drones so that it can keep a safe separation distance with the other drones. This safe separation can be achieved by a cooperative sensor system, such as the ADS-B system. In this solution, drones are equipped with GPS, an Inertial Measurement Unit (IMU), and a miniaturized transponder and they broadcast their real-time position information, which can be employed by the surrounding drones or Ground Controllers (GCs) to maintain a safe operation distance of drones at low altitude and congested airspace. In addition to ADS-B system, cooperative navigation by using Wi-Fi and other industrial, scientific, and medical (ISM) band wireless technologies have been suggested in [5] and [6]. However, these solutions do not support long ranges.

Typically, ADS-B system is susceptible to severe message collisions in dense air spaces. The random channel access of the communication protocols using the 1090 MHz frequency leads to ADS-B packet error rates above 50 percent for typical air space densities as observed during the day [1]. One of the main challenges in the employment of a cooperative sensor system, such as ADS-B, for future drone technology is packet collisions due to a larger number of drones compared to aircrafts in the airspace. As the number of drones in the airspace increases, the probability of packet collision also increases. The ADS-B system in its current form cannot handle packet collision; hence, a large number of packets are lost. Packet loss means less information and more uncertainty for the surrounding drones, resulting in less air safety.

Information extraction from collided and overlapping ADS-B packets, such as range, velocity, Angle of Arrival (AoA), etc. can contribute to safer navigation of a drone/aircraft. These

information can improve situational awareness and safety of the detect and avoid (DAA) systems. Specifically, joint ranging and phase offset (PO) estimation enables coherent detection of a single or (collided) multiple ADS-B packets with a significantly lower Packet Error Rate (PER) compared to non-coherent detection. To the best of the authors' knowledge, joint estimation of range and PO for multiple drones/aircrafts using collided ADS-B packets has not been investigated yet. Existing blind source separation algorithms suffer from sign ambiguity and require the number of receive antennas not to be larger than the number of drones/aircrafts [7], [8], [9].

In this article, we address the problem of joint range and PO estimation of multiple drones/aircrafts using the collided and overlapping ADS-B packets. We analytically derive the Maximum Likelihood (ML) cost function for joint range and PO estimation of multiple drones/aircrafts. Then, a simple solution based on the expectation–maximization (EM) algorithm is proposed. Our proposed estimator enables avionic systems employing cooperative sensors to obtain range information of the surrounding drones/aircrafts while ADS-B packet decoding is not feasible due to collision. Furthermore, the estimated range and PO can be employed for coherent detection of ADS-B packets, which offers higher detection performance. Our proposed estimator can estimate the range of multiple drones/aircrafts with a single receive antenna.

A. Related Works

Existing solutions for the separation of the overlapping ADS-B packets can be broadly divided into time-domain and spatial-domain methods [10]. The spatial-domain methods take the advantage of antenna array and if the direction of arrival of the aircrafts/drones signal are known, the signal subspace methods, such as, MUSIC [11], ESPRIT [12], and minimum variance distortionless response (MVDR) [13], can be employed for ADS-B signal separation. Projection Algorithm (PA) and corresponding extensions for the separation of the secondary surveillance radar (SSR) signal have been proposed in [14], [15]. ADS-B signal separation using high-order statistics of the received signal has shown to be ineffective because the overlapping signal is pseudo-Gaussian [16]. Furthermore, Alternating Direction Method of Multipliers (ADMM) has been suggested to solve the non-convex blind adaptive beamforming problem for ADS-B signal separation in [17]. The authors in [18] showed that the performance of the blind source separation algorithms, such as, independent component analysis (ICA) is not acceptable for ADS-B signal separation because of its short length. Principal Component Analysis (PCA) and Fast ICA algorithms for ADS-B signal separation have been proposed in [19] and [20]. A promising solution for ADS-B signal separation is Manchester decoding algorithm; however, as the delay between the reception of two ADS-B packets decreases, the performance significantly drops [18].

There are several works dealing with time-domain ADS-B signal separation. The authors in [21] have proposed to employ the empirical mode decomposition and ICA for the separation of overlapping ADS-B signals via single receive antenna. The K-means clustering for ADS-B signal separation based on

empirical mode decomposition and ICA has been developed in [22]. An anomaly doubt degree has been introduced in [23] to calculate signal overlap time delay, and adaptive threshold method based on power difference has been employed to separate ADS-B signal when the overlap signal is relatively large. The problem of ADS-B signal separation using deep learning with a single receive antenna has been investigated in [24], [25]. The authors have shown that the separation accuracy of the deep learning based algorithm is higher than that of the traditional algorithms. To the best of the authors' knowledge, the main issue with the above mentioned methods is that most of them can only separate two overlapping ADS-B signals.

B. Contributions

Consider a collection of K drones/aircrafts, which are asynchronously broadcasting ADS-B packets. This simple transmission protocol results in inevitable overlapping among multiple ADS-B signals. In this work, we show that the received complex baseband signal from these drones/aircrafts can be approximated by an independent and identically distributed (i.i.d.) Gaussian mixture (GM) random variable with 2^K mixture components in the 2D plane, which are independent of the arrival time of the ADS-B packets at the receiver. Furthermore, by using the approximate PDF, we derive the ML cost function for the joint ranging and PO estimation of multiple drones/aircrafts. We also propose the low-complexity EM-based joint ranging and PO estimation algorithm for multiple drones/aircrafts. Our proposed estimator makes active multiple target ranging possible with a single receive antenna in the presence of ADS-B packet collision. Moreover, our solution enables ADS-B systems to coherent multi-packet decoding. Finally, we extend the proposed EM-based joint estimator to the case of multiple receive antennas.

C. Notations

The identity matrix, all-zero vector, and all-one vector of length N are denoted by $\mathbf{I}_N$, $\mathbf{0}_N$, and $\mathbf{1}_N$, respectively. Throughout the article, $(\cdot)^*$, $(\cdot)^T$, and $(\cdot)^H$ show the complex conjugate, transpose, and Hermitian transpose, respectively. Also, $|\cdot|$, $\lfloor\cdot\rfloor$, $*$, and $\otimes$ represent the absolute value operator, the floor function (greatest integer value), linear convolution, and Kronecker product, respectively. $\mathbb{E}\{\cdot\}$ is the statistical expectation, $\hat{x}$ is an estimate of x. The complex Gaussian distribution with mean vector $\boldsymbol{\mu}$ and covariance matrix $\boldsymbol{\Sigma}$ is denoted by $\mathcal{CN}(\boldsymbol{\mu}, \boldsymbol{\Sigma})$. The continuous uniform distribution between a and b and the discrete uniform distribution between N_1 and N_2 are denoted by $\mathcal{U}_c[a, b]$ and $\mathcal{U}_d[N_1, N_2]$, respectively.

The remainder of the article is organized as follows. Section II introduces the system model. Section III describes the GM distribution approximation by minimizing the KLD. In Section IV, the maximum likelihood cost function and the EM-based joint ranging and PO estimation algorithm are analytically derived. Reordering estimation for the proposed EM-based joint estimator through permutation-based combinatorial optimization is investigated in Section V. Joint estimation by taking the advantage of diversity gain through multiple receive antennas is discussed in Section VI. Simulation results are provided in Section VII, and conclusions are drawn in Section VIII.
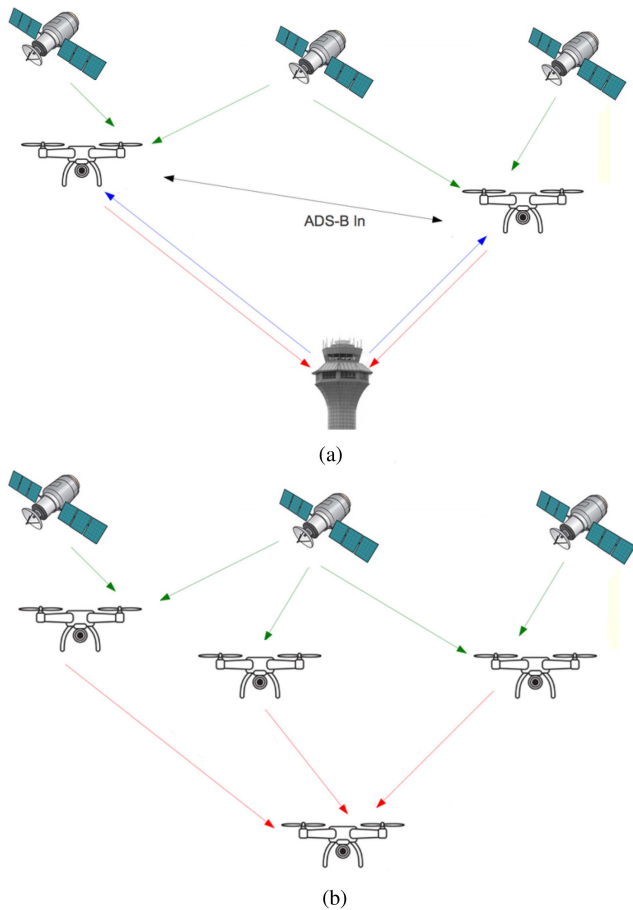
Fig. 1. Range estimation using the asynchronous ADS-B In signatures of the drones at the receiver. (a) Range estimation in a Ground Controller (GC). (b) Range estimation in a flying drone.
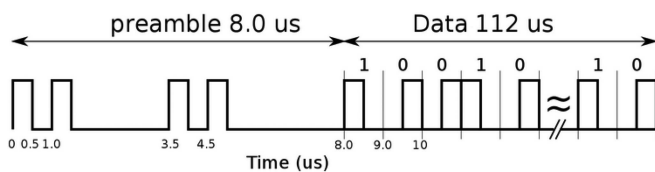

Fig. 2. ADS-B packet is composed of a preamble and data in the Pulse Position Modulation (PPM) form.

II. System Model

We consider K drones broadcasting ADS-B packets through their transponders to the GC[1] and also directly to other flying drones/aircrafts. Typical scenarios for signal reception at the GC and the flying drone are shown in Fig. 1. The packets are transmitted at 1090 MHz and use PPM at a rate of 1 Mbit per second. An ADS-B packet consists of a preamble followed by a data block is shown in Fig. 2.

It is assumed that the drones/aircrafts asynchronously broadcast their ADS-B packets every T_P seconds. We consider an

Fig. 3. Reception of the ADS-B packets at the receiver. Drones periodically broadcast ADS-B packets. Different colors are used to show the packet of drones. (a) The received ADS-B packet at the receiver and the observation window with length T_w. (b) A special case where the complete ADS-B packets of all the drones fall inside the observation window with length T_w.

observation window of length $T_w = T_P$ for parameter estimation at the receiver (Fig. 3(a)). To make the joint ranging and PO estimation independent of the arrival time of the ADS-B packets at the receiver, we approximate the received samples in the observation interval by an i.i.d. complex random variable as it will be explained in Section III. Hence, without loss of generality, we can consider the ADS-B packet reception in Fig. 3(b) to simplify modeling of the joint range and PO estimation. In this case, it is assumed that the ADS-B packet of the kth drone/aircraft with a packet length of T_A is received at the receiver with time delay $\tau_k \in [0, \tau_{\max}]$ in the timing reference of the receiver, where τ_k is unknown and random in each observation window of length $T_w = T_P$, and $\tau_{\max} = T_P - T_A$ is the maximum time delay of a packet.

By employing a baseband low pass filter with sufficient bandwidth B at the receiver after RF down-conversion, the received complex baseband signal at the ADS-B receiver can be expressed as

$$y(t) \approx \sum_{k=1}^{K} \sqrt{P_k L_k} x_k(t - \tau_k) e^{j(2\pi \Delta f_k t + \theta_k)} + w(t), \quad (1)$$

where $t \in [0, T_w]$, and where P_k, $x_k(t)$, $w(t)$, and L_k denote, the transmit power by the kth drone, the transmit PPM waveform by the kth drone, the additive noise with Power Spectral Density (PSD) N_0 over the frequency $f \in [-B, B]$, and the path loss between the kth drone/aircraft and the ADS-B receiver, respectively. For free-space path loss, we have

$$L_k \triangleq \left(\frac{\lambda_c}{4\pi r_k} \right)^2, \quad (2)$$

---

[1] The GC can be a simple Software-defined Radio (SDR) receiver. Number of drones/aircrafts, K, can be determined by employing model-order selection techniques [26], [27] prior to joint ranging and PO estimation.
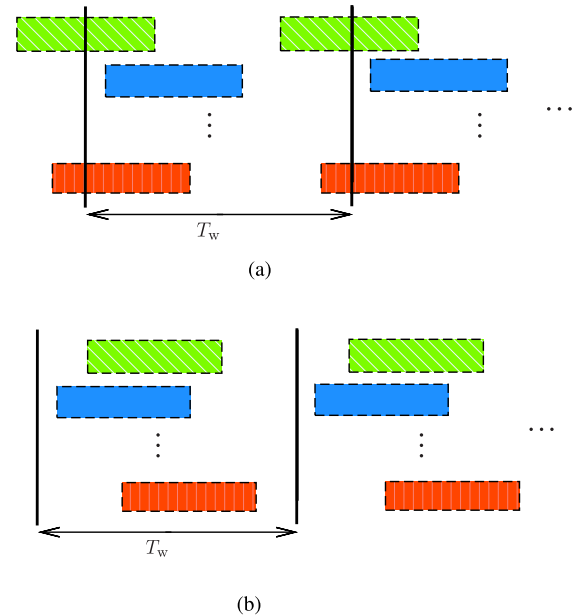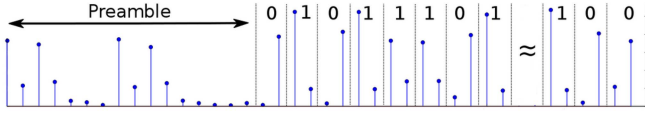
Fig. 4.   Amplitude of the noisy ADS-B packet after sampling.

where r_k is the range between the kth drone and the receiver, $\lambda_c \triangleq c/f_c$ is the wavelength of the carrier wave, c denotes the speed of light, and f_c represents the carrier frequency. For the ADS-B system, since $f_c = 1090$ MHz, we have $\lambda_c \approx 0.2752$ m. In (1), Δf_k and θ_k further denote the Carrier Frequency Offset (CFO) and the electrical PO of the kth drone in the observation window. The CFO and PO occur because the local oscillator signal for RF down-conversion at the receiver does not synchronize with the carrier signal.[2]

In this article, we consider that $\Delta f_k T_w \ll 1$ and $\exp(j2\pi\Delta f_k t) \approx 1$ for $t \in [0, T_w]$, $k = 1, 2, \ldots, K$; thus, we can write

$$y(t) \approx \sum_{k=1}^{K} \sqrt{P_k L_k} x_k(t - \tau_k) e^{j\theta_k} + w(t). \qquad (3)$$

Assumption 1: We assume that $P_k, k = 1, 2, \ldots, K,$ is known at the receiver, and that $P_1 L_1 > P_2 L_2 > \ldots, P_K L_K$.

Since the bit-rate for ADS-B systems is 1M bit/s, a sampling rate of $f_s = \frac{1}{T_s} = 2\text{M samples/s}$ is sufficient to capture the bit transitions, detect the preamble and decode packets. A typical sampled ADS-B signal is shown in Fig. 4 for visualization. The discrete-time received baseband signal after sampling, i.e., $y_n \triangleq y(nT_s), n = 0, 1, \ldots, N,$ where $N = 239 + M,$[3] $M \triangleq \lfloor \frac{\tau_{\max}}{T_s} \rfloor,$ can be written in vector form as

$$\mathbf{y} = \sum_{k=1}^{K} h_k \mathbf{x}_k + \mathbf{w} = \sum_{k=1}^{K} \mathbf{z}_k + \mathbf{w} = \mathbf{g} + \mathbf{w}, \qquad (4)$$

where $\mathbf{g} \triangleq \sum_{k=1}^{K} h_k \mathbf{x}_k = \sum_{k=1}^{K} \mathbf{z}_k,$ $\mathbf{z}_k = h_k \mathbf{x}_k,$

$$\mathbf{y} \triangleq \begin{bmatrix} y_0 \ y_1 \ \cdots \ y_N \end{bmatrix}^T, \qquad (5a)$$

$$\mathbf{g} \triangleq \begin{bmatrix} g_0 \ g_1 \ \cdots \ g_N \end{bmatrix}^T, \qquad (5b)$$

$$\mathbf{w} \triangleq \begin{bmatrix} w_0 \ w_1 \ \cdots \ w_N \end{bmatrix}^T, \qquad (5c)$$

$$\mathbf{z}_k \triangleq \begin{bmatrix} z_{k,0} \ z_{k,1} \ \cdots \ z_{k,N} \end{bmatrix}^T, \qquad (5d)$$

$w_n \triangleq w(nT_s), h_k \triangleq \beta_k e^{j\theta_k}, \beta_k \triangleq \sqrt{P_k L_k},$ and

$$\mathbf{x}_k \triangleq \begin{bmatrix} x_{k,0} \ x_{k,1} \ \cdots \ x_{k,N} \end{bmatrix}^T$$
$$\triangleq \begin{bmatrix} \mathbf{0}_{m_k}^T \ \mathbf{s}^T \ \mathbf{d}_k^T \ \mathbf{0}_{M-m_k}^T \end{bmatrix}^T. \qquad (6)$$

In (6), $x_{k,n} \triangleq x_k(nT_s - \tau_k), \mathbf{d}_k \in \{0, 1\}^{224},$ is the PPM data vector of the kth drone with a length of 224 symbols, $\mathbf{s}$ is the preamble vector given by $\mathbf{s} = \begin{bmatrix} 1\,0\,1\,0\,0\,0\,0\,0\,1\,0\,1\,0\,0\,0\,0 \end{bmatrix}^T,$

2The tolerable PO estimation error for coherent ADS-B detection depends on the value of SNR. The higher value of SNR, the less sensitivity to the PO estimation error in coherently detecting an ADS-B packet.

3A sampling rate of 2M samples/s results in 240 samples per ADS-B packet.

and $M \triangleq \lfloor \frac{\tau_{\max}}{T_s} \rfloor$ and $m_k \triangleq \lfloor \frac{\tau_k}{T_s} \rfloor$ denote the maximum possible integer delay for a drone/aircraft and the integer delay of the kth drone/aircraft, respectively. The integer delays $m_k, k = 1, 2, \ldots, K,$ are unknown at the receiver and their values change from one observation window to another. The vector $\mathbf{w} \triangleq \begin{bmatrix} w_0 \ w_1 \ \ldots \ w_N \end{bmatrix}^T$ in (4) denotes the additive white Gaussian noise (AWGN) with covariance matrix $\mathbb{E}\{\mathbf{w}\mathbf{w}^T\} = \sigma_w^2 \mathbf{I} = 2N_0 B\mathbf{I}$.

Let us define hypothesis H_m^k as follows:

$$H_m^k: \quad \mathbf{x}_k = \begin{bmatrix} \mathbf{0}_m^T, \mathbf{s}^T, \mathbf{d}_k^T, \mathbf{0}_{M-m}^T \end{bmatrix}^T, \qquad (7)$$

which represents the ADS-B packet of the kth drone arriving at the receiver with integer delay $m_k = m \in \{0, 1, \ldots, M\}$.

III. DISTRIBUTION APPROXIMATION

To remove the dependency of joint ranging and PO estimation from the unknown arrival time of the ADS-B packets at the receiver, we approximate the received noisy samples in the observation interval by i.i.d. complex random variables. In this article, we show that an i.i.d. two-dimensional (2D) GM model can be used to model the received baseband superimposed and noise corrupted signal at the receiver.

Theorem 1: By maximizing the KLD criterion, the elements of the ADS-B packet of the kth drone, i.e., $\mathbf{x}_k = \begin{bmatrix} x_{k,0} \ x_{k,1} \ \ldots \ x_{k,N} \end{bmatrix}^T = \begin{bmatrix} \mathbf{0}_{m_k}^T \ \mathbf{s}^T \ \mathbf{d}_k^T \ \mathbf{0}_{M-m_k}^T \end{bmatrix}^T$ can be approximated by an i.i.d. random variable that are Bernoulli distributed with Probability Mass Function (PMF)

$$q(x; p) = \begin{cases} p & \text{if } x = 0, \\ 1 - p & \text{if } x = 1, \end{cases} \qquad (8)$$

where

$$p = \frac{M + 124}{M + 240}. \qquad (9)$$

Proof: See Appendix A. $\square$

As seen in Theorem 1, the approximated PMF q does not depend on H_m^k.

Since $\mathbf{z}_k = h_k \mathbf{x}_k$ is the scaled version of $\mathbf{x}_k$ and the parameter of the Bernoulli distribution, p, is independent of m_k, the elements of the complex vector $\mathbf{z}_k$ can be approximated by i.i.d. complex random variables Z_k with PDF $f_{Z_k}(z; p, h_k)$ as follows

$$f_{Z_k}(z; p, h_k) = p\delta_c(z) + (1 - p)\delta_c(z - h_k), \qquad (10)$$

where $\delta_c(z), z = z_r + jz_I \in \mathbb{C},$ is the complex Delta function and is defined as

$$\delta_c(z) \triangleq \delta(z_r)\delta(z_I), \qquad (11)$$

where $\delta(t), t \in \mathbb{R},$ is the Dirac Delta function.

We consider that $g_i \triangleq \sum_{k=1}^{K} z_{k,i} \sim G$ and $z_{k,i} \sim Z_k$ given in (10), where the symbol $\sim$ denotes distributed according to. The PDF of the sum of independent random variables is obtained as the convolution of the PDFs. For the complex random variable, $G = \sum_{k=1}^{K} Z_k$, by employing the multi-binomial theorem [28],

we can obtain the PDF of G as

$$f_G(g; p, \mathbf{h}) = \sum_{v_1=0}^{1} \cdots \sum_{v_K=0}^{1} \left[p^{\sum_{k=1}^{K} v_k} (1-p)^{K-\sum_{k=1}^{K} v_k} \right.$$

$$\left. \times \delta_c \left(g - \sum_{k=1}^{K} (1-v_k) h_k \right) \right], \qquad (12)$$

where $\mathbf{h} \triangleq [h_1, h_2, \ldots, h_K]^T$.

Proof: See Appendix B. $\qquad\qquad\square$

For the circularly symmetric complex Gaussian noise vector, $\mathbf{w} \triangleq [w_0 \ w_1 \ \ldots \ w_N]^T$, the PDF of the random variable W associated with the noise elements is expressed as

$$f_W(w; \sigma_w^2) \triangleq \frac{1}{\pi \sigma_w^2} \exp\left(\frac{-|w|^2}{\sigma_w^2} \right), \qquad (13)$$

where $w \in \mathbb{C}$. From (4), we have $y_n = g_n + w_n$, $n = 0, 1, \ldots, N$, where $g_n \sim G$ and $w_n \sim W$. Since G and W are independent complex random variables, the PDF of $Y = G + W$ is obtained by the linear convolution of the PDFs in (12) and (13), which results in

$$f_Y(y; p, \boldsymbol{\beta}, \boldsymbol{\theta}, \sigma_w^2) = \sum_{a=0}^{2^K-1} \frac{\xi_a}{\pi \sigma_w^2} \mathcal{CN}(y; \mu_a, \sigma_w^2)$$

$$= \sum_{a=0}^{2^K-1} \frac{\xi_a}{\pi \sigma_w^2} \exp\left(-\frac{|y - \mu_a|^2}{\sigma_w^2} \right), \qquad (14)$$

where

$$\boldsymbol{\beta} \triangleq [\beta_1 \ \beta_2 \ \ldots \ \beta_K]^T, \qquad (15a)$$

$$\boldsymbol{\theta} \triangleq [\theta_1 \ \theta_2 \ \ldots \ \theta_K]^T, \qquad (15b)$$

$$\xi_a \triangleq p^{\sum_{k=1}^{K} b_k} (1-p)^{K-\sum_{k=1}^{K} b_k}, \qquad (16)$$

and

$$\mu_a \triangleq \sum_{k=1}^{K} (1-b_k) h_k = \sum_{k=1}^{K} (1-b_k) \beta_k \exp(j\theta_k) \qquad (17)$$

with b_i the ith bit in the binary representation of a as

$$a = (b_K, b_{K-1}, \ldots, b_1)_2, \qquad b_i \in \{0, 1\}, \qquad (18)$$

and $a = 0, 1, \ldots, 2^K - 1$.

As seen, $f_Y(y; p, \boldsymbol{\beta}, \boldsymbol{\theta}, \sigma_w^2)$ represents a 2D GM, where its modes are located at the delta functions given in (12). Since $\theta_1, \theta_2, \ldots, \theta_K$, are independent uniform random variables in the range of $[0, 2\pi)$, and $\beta_1 > \beta_2 > \ldots > \beta_K$, with probability of almost one, the number of distinct mixtures is 2^K. Fig. 5 illustrates the constellation of the received signal for $K = 3$ drones, maximum integer delay $M = 20$, and transmit power of 51 dBm.
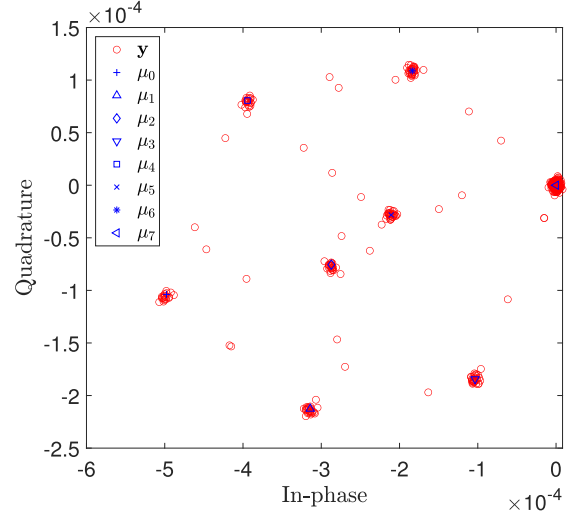

Fig. 5. In-phase and quadrature components of the received signal for $K = 3$ drones at $r_1 = r_2 = r_3 = 12$ Km with transmit power of 51 dBm.

IV. JOINT RANGE AND PO ESTIMATION

The MLE for the vector parameters $[\boldsymbol{\beta}^T \ \boldsymbol{\theta}^T]^T$ given observation vector $\mathbf{y} = [y_0 \ y_2 \ \ldots \ y_N]^T$ is expressed as

$$\{\hat{\boldsymbol{\beta}}, \hat{\boldsymbol{\theta}}\} = \arg\max_{\boldsymbol{\beta}, \boldsymbol{\theta}} \sum_{n=0}^{N} \ln f_Y(y_n; p, \boldsymbol{\beta}, \boldsymbol{\theta}, \sigma_w^2). \qquad (19)$$

The maximization problem in (19) cannot be analytically solved in a trackable manner. An alternative simple solution is to employ the EM algorithm to estimate the 2^K modes of the GM components; then, we can decouple the desired parameters, i.e., $\boldsymbol{\beta}$ and $\boldsymbol{\theta}$ from the estimated modes.

Let $\boldsymbol{\mu} \triangleq [\mu_0 \ \mu_1 \ \ldots \ \mu_{2^K-1}]^T$ denote the mode vector of the GM, where μ_a, $a = 0, 1, \ldots, 2^K - 1$, is given by (17). The elements of the vector $\boldsymbol{\mu}$ for $K = 2, 3, 4$ are given in Appendix C.

Let us define the discrete function $\chi_q(n)$ as

$$\chi_q(n) : \{1, 2, \ldots, l\} \longrightarrow \{1, 2, \ldots, l\}, \qquad (20)$$

where for $n_1 \neq n_2$, $\chi_q(n_1) \neq \chi_q(n_2)$. There are $Q_l \triangleq l!$ unique functions in the form of (20), where ! denotes the factorial function. Using (20), Q_l permutation matrices of size $l \times l$ can be defined as

$$\boldsymbol{\Lambda}_q = \begin{bmatrix} \mathbf{e}_{\chi_q(1)} \\ \mathbf{e}_{\chi_q(2)} \\ \vdots \\ \mathbf{e}_{\chi_q(l)} \end{bmatrix}, \qquad (21)$$

where $\mathbf{e}_\ell$, $\ell = 1, 2, \ldots, l$, denote the standard basis vectors of length l with a 1 in the ℓth coordinate and 0's elsewhere. The set composed of all permutations of vector $\mathbf{a} = [a_1 \ a_2 \ \ldots \ a_l]^T$ is given by

$$\mathcal{F}_{\mathbf{a}}^{Q_l} \triangleq \{\boldsymbol{\Lambda}_1 \mathbf{a}, \boldsymbol{\Lambda}_2 \mathbf{a}, \ldots, \boldsymbol{\Lambda}_{Q_l} \mathbf{a}\}, \qquad (22)$$

where $Q_l = l!$.

The EM algorithm estimates the permuted mode vector $\boldsymbol{\eta} = [\eta_0\,\eta_1\,\ldots\,\eta_{2^K-1}]^T \in \mathcal{F}_{\boldsymbol{\mu}}^{Q_{2^K}} \subset \mathbb{C}^{2^K}$, where $Q_{2^K} = 2^K!$ and $\boldsymbol{\mu} \triangleq [\mu_0\,\mu_1\,\ldots\,\mu_{2^K-1}]^T$. The EM algorithm defines a latent random vector $\mathbf{u} \triangleq [u_0\,u_1\,\ldots\,u_N]^T$ that determines the GM component from which the observation originates, i.e., $f_{Y|U}(y_n|u_n = a; p, \boldsymbol{\beta}, \boldsymbol{\theta}, \sigma_w^2) \sim \mathcal{CN}(y_n; \mu_a, \sigma_w^2)$, where $P_U(u_n = a) = \xi_a$ for $n = 0, 1, \ldots, N$ and $a = 0, 1, \ldots, 2^K - 1$. The EM algorithm iteratively maximizes the expected value of the complete-data log-likelihood function to estimate the permuted mode vector $\boldsymbol{\eta} = [\eta_0\,\eta_1\,\ldots\,\eta_{2^K-1}]^T \in \mathcal{F}_{\boldsymbol{\mu}}^{Q_{2^K}} \subset \mathbb{C}^{2^K}$ of the GM as follows [29], [30], [31]

$$\hat{\boldsymbol{\eta}}^{(t+1)} = \arg\max_{\boldsymbol{\eta}} Q(\boldsymbol{\eta}|\boldsymbol{\eta}^{(t)}), \tag{23}$$

where $\boldsymbol{\eta}^{(0)}$ is the initialization vector,

$$Q(\boldsymbol{\eta}|\boldsymbol{\eta}^{(t)}) = \mathbb{E}_{\boldsymbol{U}|\boldsymbol{Y},\boldsymbol{\eta}^{(t)}}\left\{\ln f_{\boldsymbol{Y},\boldsymbol{U}}\left(\mathbf{y}, \mathbf{u}; p, \boldsymbol{\eta}, \sigma_w^2\right)\right\}$$

$$= \sum_{n=0}^{N}\sum_{a=0}^{2^K-1} \lambda_{a,n}^{(t)}\left(\ln\frac{\xi_a}{\pi\sigma_w^2} - \frac{|y_n - \eta_a|^2}{\sigma_w^2}\right), \tag{24}$$

with

$$\lambda_{a,n}^{(t)} = P_{U|Y}\left(u_n = a|y_n; \boldsymbol{\eta}^{(t)}\right)$$

$$= \frac{P_U(u_n = a)f_{Y|U}\left(y_n|u_n = a; \boldsymbol{\eta}^{(t)}\right)}{f_Y(y_n)}$$

$$= \frac{\xi_a\mathcal{CN}\left(y_n; \eta_a^{(t)}, \sigma_w^2\right)}{\sum_{q=0}^{2^K-1}\xi_q\mathcal{CN}\left(y_n; \eta_q^{(t)}, \sigma_w^2\right)}, \tag{25}$$

and the complete-data likelihood function is given by

$$f_{\boldsymbol{Y},\boldsymbol{U}}\left(\mathbf{y}, \mathbf{u}; p, \boldsymbol{\eta}, \sigma_w^2\right) = \prod_{n=0}^{N}\prod_{a=0}^{2^K-1}\left(\xi_a\mathcal{CN}\left(y_n; \eta_a, \sigma_w^2\right)\right)^{\mathbb{I}\{u_n=a\}}. \tag{26}$$

In (26), $\mathbb{I}\{\cdot\}$ denotes the indicator function, and ξ_a is a function of p and is given in (16). The EM algorithm at the $(t+1)$th iteration estimates the vector $\boldsymbol{\eta}^{(t+1)} = [\eta_0^{(t+1)}\,\eta_1^{(t+1)}\,\ldots\,\eta_{2^K-1}^{(t+1)}]^T$ which is a permuted version of the vector $\boldsymbol{\mu}$. The order of $\boldsymbol{\eta}^{(t+1)}$ depends on the initialization of the EM algorithm, i.e., $\boldsymbol{\eta}^{(0)}$. By solving the maximization problem in (23), the elements of $\boldsymbol{\eta}^{(t+1)}$ are iteratively updated as follows

$$\eta_a^{(t+1)} = \frac{\sum_{n=0}^{N}\lambda_{a,n}^{(t)}y_n}{\sum_{n=0}^{N}\lambda_{a,n}^{(t)}}, \tag{27}$$

for $a = 0, 1, \ldots, 2^K - 1$, where the convergence condition for the EM algorithm is $\|\boldsymbol{\eta}^{(t+1)} - \boldsymbol{\eta}^{(t)}\| < \epsilon$, with ϵ a preset threshold. We denote $\hat{\boldsymbol{\eta}} = \boldsymbol{\eta}^{(t+1)}$ when the EM algorithm converges at the $(t+1)$th iteration.

The EM algorithm may converge to a local maximum of the observed data likelihood function, depending on the starting value. A variety of heuristic or metaheuristic approaches exist to escape a local maximum, such as random-restart hill climbing where the EM algorithm starts with different random initial estimates. The recursive expression in (27) is very straightforward and can be easily computed for multiple initial points.

Hence, EM with random-restart hill climbing can be employed for the problem at hand. As mentioned earlier, there is an order ambiguity in the vector $\hat{\boldsymbol{\eta}}$; thus, reordering estimation is required to resolve this ambiguity. In the next section, we propose different solutions based on permutation- based combinatorial optimization for one to one mapping between the elements of $\hat{\boldsymbol{\eta}}$ and $\boldsymbol{\mu}$.

V. REORDERING ESTIMATION

The goal of reordering estimation is to change the order of the elements in $\hat{\boldsymbol{\eta}} \triangleq [\hat{\eta}_0\,\hat{\eta}_1\,\ldots\,\hat{\eta}_{2^K-1}]^T$, obtained by the EM algorithm, to achieve a new vector $\hat{\boldsymbol{\mu}} \triangleq [\hat{\mu}_0\,\hat{\mu}_1\,\ldots\,\hat{\mu}_{2^K-1}]^T$ that corresponds to an estimate of $\boldsymbol{\mu} \triangleq [\mu_0\,\mu_1\,\ldots\,\mu_{2^K-1}]^T$. Let us denote $\hat{\eta}_i$ as the element of $\hat{\boldsymbol{\eta}}$ that corresponds to $\mu_{2^K-1} = 0$. The index i can be estimated as

$$|\hat{\eta}_i| < \min\left\{|\hat{\eta}_0|, |\hat{\eta}_1|, \ldots, |\hat{\eta}_{i-1}|, |\hat{\eta}_{i+1}|, \ldots, |\hat{\eta}_{2^K-1}|\right\}. \tag{28}$$

Accordingly, we have $\hat{\mu}_{2^K-1} = \hat{\eta}_i$. Let us now define

$$\hat{\boldsymbol{\eta}}_i \triangleq [\hat{\eta}_0\,\hat{\eta}_1\,\ldots\,\hat{\eta}_{i-1}\,\hat{\eta}_{i+1}\,\ldots\,\hat{\eta}_{2^K-1}]^T, \tag{29}$$

and

$$\hat{\mathcal{A}}_l \triangleq \Big\{[\phi_1\,\phi_2\,\ldots\,\phi_l]^T | \forall d \in \{1, 2, \ldots, l\},$$

$$\phi_d \in \{\hat{\eta}_0, \hat{\eta}_1, \ldots\,\hat{\eta}_{i-1}, \hat{\eta}_{i+1}\,\ldots\,\hat{\eta}_{2^K-1}\},$$

$$|\phi_1| > |\phi_2| > \ldots|\phi_l|\Big\}. \tag{30}$$

Different reordering estimation methods for $\hat{\boldsymbol{\beta}}$ and $\hat{\boldsymbol{\theta}}$ can be considered. The Least Squares (LS) reordering estimation for $\hat{\boldsymbol{\beta}}$ and $\hat{\boldsymbol{\theta}}$ form $\hat{\boldsymbol{\eta}}_i$ is given by

$$\hat{\mathbf{h}} = \hat{\boldsymbol{\beta}}e^{j\hat{\boldsymbol{\theta}}} = \hat{\boldsymbol{\Lambda}}\mathbf{A}\hat{\boldsymbol{\Phi}}, \tag{31}$$

where

$$\{\hat{\Lambda}, \hat{\boldsymbol{\Phi}}\} = \arg\min_{\boldsymbol{\Lambda},\boldsymbol{\Phi}}\left\|\boldsymbol{\Lambda}\mathbf{A}\boldsymbol{\Phi} - \hat{\boldsymbol{\eta}}_i\right\|_2,$$

$$\text{s.t. } \boldsymbol{\Phi} \triangleq [\Phi_1, \Phi_2, \ldots, \Phi_K]^T \in \hat{\mathcal{A}}_K$$

$$\boldsymbol{\Lambda} \in \{\boldsymbol{\Lambda}_1, \boldsymbol{\Lambda}_2, \ldots, \boldsymbol{\Lambda}_{(2^K-1)!}\} \tag{32}$$

where $\boldsymbol{\Lambda}_i$ is a permutation matrix of size $2^{K-1} \times 2^{K-1}$ given in (21) for $l = 2^{K-1}$, and $\mathbf{A}$ is the $2^{K-1} \times K$ matrix given by

$$\mathbf{A} \triangleq \begin{bmatrix} \mathbf{e}_1 \\ \mathbf{e}_2 \\ \vdots \\ \mathbf{e}_K \\ \mathbf{e}_1 + \mathbf{e}_2 \\ \mathbf{e}_1 + \mathbf{e}_3 \\ \vdots \\ \mathbf{e}_1 + \mathbf{e}_2 + \ldots + \mathbf{e}_K \end{bmatrix}, \tag{33}$$

where $\mathbf{e}_j$, $j = 1, 2, \ldots, K$, denote the standard basis vectors of length K.

An alternative minimization problem with lower computational complexity for vector reordering is given by

$$\{\hat{\mathbf{\Lambda}}, \hat{\mathbf{\Phi}}\} = \arg \min_{\mathbf{\Lambda}, \mathbf{\Phi}} \|\mathbf{\Lambda}\mathbf{A}\mathbf{\Phi} - \hat{\boldsymbol{\eta}}_i\|_2,$$

$$\text{s.t. } \mathbf{\Phi} \triangleq [\Phi_1, \Phi_2, \ldots, \Phi_K]^T \in \mathbb{C}^K$$

$$\mathbf{\Lambda} \in \{\mathbf{\Lambda}_1, \mathbf{\Lambda}_2, \ldots, \mathbf{\Lambda}_{(2^{K-1})!}\} \quad (34)$$

By employing the solution of the unconstrained LS minimization for a linear observation model [32] and the fact that $\mathbf{\Lambda}^T\mathbf{\Lambda} = \mathbf{\Lambda}\mathbf{\Lambda}^T = \mathbf{I}_{2^K-1}$, we can easily write

$$\mathbf{\Phi} = (\mathbf{A}^T\mathbf{A})^{-1}\mathbf{A}^T\mathbf{\Lambda}^T\hat{\boldsymbol{\eta}}_i, \quad (35)$$

and thus we can formulate the following problem

$$\hat{\mathbf{\Lambda}} = \arg \min_{\mathbf{\Lambda}} \hat{\boldsymbol{\eta}}_i^T(\hat{\boldsymbol{\eta}}_i - \mathbf{\Lambda}\mathbf{A}\mathbf{\Phi})$$

$$\text{s.t. } \mathbf{\Phi} = (\mathbf{A}^T\mathbf{A})^{-1}\mathbf{A}^T\mathbf{\Lambda}^T\hat{\boldsymbol{\eta}}_i$$

$$|\Phi_1| > |\Phi_2| > \ldots > |\Phi_K|$$

$$\mathbf{\Lambda} \in \{\mathbf{\Lambda}_1, \mathbf{\Lambda}_2, \ldots, \mathbf{\Lambda}_{(2^{K-1})!}\}. \quad (36)$$

Our simulation experiments show that for low and moderate Signal-to-Noise Ratios (SNRs), the vector reordering based on the combinatorial optimization in (34) outperforms the one in (32) in terms of estimation error. While the vector reordering based on the minimization formulation in (34) offers a lower computational complexity compared to the minimization in (32), the computational complexity of both methods is still high for $K > 4$.

An alternative low complexity solution is to define a combinatorial optimization with lower cardinality. By selecting all Q-combination of the set $\{\hat{\eta}_0 \ \hat{\eta}_1 \ \ldots \ \hat{\eta}_{i-1} \ \hat{\eta}_{i+1} \ \ldots \ \hat{\eta}_{2^K-1}\}$, we can define a $C_Q^{2^K-1}$-cardinality combinatorial optimization problem that minimizes a linear/non-linear combinations of the elements in the set in such a way that one or more elements of the set can be unambiguously assigned to the elements of $\boldsymbol{\mu}$.

As an example, for $K = 4$ drones/aircrafts, our goal is to estimate $\mu_{14} = \beta_1 \exp(j\theta_1)$, $\mu_{13} = \beta_2 \exp(j\theta_2)$, $\mu_{11} = \beta_3 \exp(j\theta_3)$, and $\mu_7 = \beta_4 \exp(j\theta_4)$, where $\beta_1 > \beta_2 > \beta_3 > \beta_4$ (refer to (70)). We can easily show that there is a unique solution for the linear equation

$$z_0 + z_1 + z_2 + z_3 - z_4 = 0, \quad (37)$$

where $z_i \in \{\mu_0 \ \mu_1 \ \ldots \ \mu_{14}\}$ and $|z_1| > |z_2| > |z_3| > |z_4|$. This unique solution is $\mu_{14} + \mu_{13} + \mu_{11} + \mu_7 - \mu_0 = 0$, where $\mu_0 = \sum_{i=1}^4 \beta_i \exp(j\theta_i)$, $\mu_{14} = \beta_1 \exp(j\theta_1)$, $\mu_{13} = \beta_2 \exp(j\theta_2)$, $\mu_{11} = \beta_3 \exp(j\theta_3)$, and $\mu_7 = \beta_4 \exp(j\theta_4)$ for $\beta_1 > \beta_2 > \beta_3 > \beta_4$. By taking this into account, we can define the following combinatorial optimization for reordering estimation

$$\hat{\mathbf{\Phi}} = \arg \min_{\mathbf{\Phi}} |\mathbf{v}^T \mathbf{\Phi}|$$

$$\text{s.t. } \mathbf{\Phi} \triangleq [\phi_1 \ \phi_2 \ \ldots \ \phi_5]^T \in \hat{\mathcal{A}}_5 \quad (38)$$

where $\hat{\mathbf{\Phi}} \triangleq [\hat{\phi}_1 \ \hat{\phi}_2 \ \ldots \ \hat{\phi}_5]^T$, the set $\hat{\mathcal{A}}_5$ is defined in (30) for $l = 5$, and $\mathbf{v} \triangleq [v_1 \ v_2 \ v_3 \ v_4 \ v_5]^T = [1 \ 1 \ 1 \ 1 \ -1]^T$. It is obvious that (38) represents a $C_5^{15} = 3003$-cardinality combinatorial optimization problem. By solving the combinatorial optimization

in (38), we obtain

$$\hat{\mathbf{h}} = \hat{\boldsymbol{\beta}}e^{j\hat{\boldsymbol{\theta}}} = [\hat{\phi}_1 \ \hat{\phi}_2 \ \hat{\phi}_3 \ \hat{\phi}_4]^T. \quad (39)$$

Different combinatorial optimization problems can be defined for reordering estimation. For $K = 4$, let us consider the following linear equation

$$7\sum_{i=0}^3 z_i - \sum_{i=4}^{14} z_i = 0, \quad (40)$$

where $z_i \in \{\mu_0 \ \mu_1 \ \ldots \ \mu_{14}\}$ and $|z_1| > |z_2| > |z_3| > |z_4|$. Since $\beta_1 > \beta_2 > \beta_3 > \beta_4$ (refer to Assumption 1), we can show that the solution of (40) is given by $7\mu_{14} + 7\mu_{13} + 7\mu_{11} + 7\mu_7 - \mathbf{c}^T\mathbf{\Lambda}^T = 0$, where $\mathbf{c} \triangleq [\mu_0 \ \mu_1 \ \mu_2 \ \mu_3 \ \mu_4 \ \mu_5 \ \mu_6 \ \mu_8 \ \mu_9 \ \mu_{10} \ \mu_{12}]^T$ and $\mathbf{\Lambda}$ is a 11×11 permutation matrix.[4] Taking this equation into account, the combinatorial optimization for reordering estimation can be expressed as

$$\hat{\mathbf{\Phi}} = \arg \min_{\mathbf{\Phi}} \left|7\mathbf{\Phi}^T\mathbf{1}_4 - \alpha\right|,$$

$$\text{s.t. } \mathbf{\Phi} \triangleq [\phi_1 \ \phi_2 \ \phi_3 \ \phi_4]^T \in \hat{\mathcal{A}}_4$$

$$\alpha = \sum_{\kappa \in \mathcal{S}} \kappa \quad (41)$$

where $\mathcal{S} \triangleq \{\hat{\eta}_0, \hat{\eta}_1, \ldots \ \hat{\eta}_{i-1}, \hat{\eta}_{i+1} \ \ldots \ \hat{\eta}_{2^K-1}\} - \{\phi_1, \phi_2, \phi_3, \phi_4\}$, $\hat{\mathbf{\Phi}} \triangleq [\hat{\phi}_1 \ \hat{\phi}_2 \ \hat{\phi}_3 \ \hat{\phi}_4]^T$, $\mathbf{1}_4 = [1 \ 1 \ 1 \ 1]^T$, and the set $\hat{\mathcal{A}}_4$ is defined in (30) for $l = 4$. By using the solution of the minimization in (41), we can write $\hat{\mathbf{h}} = \hat{\boldsymbol{\beta}}e^{j\hat{\boldsymbol{\theta}}} = [\hat{\phi}_1 \ \hat{\phi}_2 \ \hat{\phi}_3 \ \hat{\phi}_4]^T$.

It should be mentioned that other combinatorial optimizations can also be defined for reordering estimation. Ambiguity removal through multiple combinatorial optimization problems can also be considered.

A. Joint Range and PO Estimation

For joint range and PO estimation of K drones, the modes $\mu_{a_k} \triangleq \sqrt{P_k L_k}e^{j\theta_k}$, $k = 1, 2, \ldots, K$, are needed to be estimated, where

$$a_k = \sum_{\substack{n=0 \\ n \neq k-1}}^{K-1} 2^n. \quad (42)$$

Let $\hat{\mu}_{a_k}$, $k = 1, 2, \ldots, K$, denote the estimated modes after reordering estimation. By using (2), the range and PO for the kth drone are estimated as

$$\hat{r}_k = \frac{\lambda_c \sqrt{P_k}}{|4\pi\hat{\mu}_{a_k}|}, \quad (43)$$

and

$$\hat{\theta}_k = \begin{cases} \tan^{-1} \frac{\Im\{\hat{\mu}_{a_k}\}}{\Re\{\hat{\mu}_{a_k}\}}, & \Re\{\hat{\mu}_{a_k}\} \geq 0 \\ \tan^{-1} \frac{\Im\{\hat{\mu}_{a_k}\}}{\Re\{\hat{\mu}_{a_k}\}} + \pi, & \Re\{\hat{\mu}_{a_k}\} < 0 \end{cases}. \quad (44)$$

where $\Im\{\cdot\}$ and $\Re\{\cdot\}$ denotes the real and imaginary operators, respectively. The proposed EM-based joint ranging and PO

---

[4]The second summation is independent of the permutation of $\mathbf{c}$.

Algorithm 1: EM-Based Joint Ranging and PO Estimation.

> **Input:** $P_1, P_2, \ldots, P_K$ and $\mathbf{y}$
> **Output:** $\hat{r}_k$ and $\hat{\theta}_k$ for $k = 1, 2, \ldots, K$
> Initialize $\boldsymbol{\eta}^{(0)}$
> 1: **for** $t = 0, 1, \ldots, T_{\mathrm{EM}} - 1$ **do**
> 2: Use (27) to obtain
> $\boldsymbol{\eta}^{(t+1)} \triangleq [\eta_0^{(t+1)} \; \eta_1^{(t+1)} \; \cdots \; \eta_{2^K-1}^{(t+1)}]^T$
> 3: **if** $\|\boldsymbol{\eta}^{(t+1)} - \boldsymbol{\eta}^{(t)}\| < \epsilon$ or $t = T_{\mathrm{EM}} - 1$
> 4: $\hat{\boldsymbol{\eta}} = \boldsymbol{\eta}^{(t+1)}$ and $t = T_{\mathrm{EM}}$
> 5: **end if**
> 6: **end for**
> 7: Use (28) to estimate the element of $\hat{\boldsymbol{\eta}}$ that corresponds to $\mu_{2^K-1} = 0$ and obtain $\hat{\eta}_i$ in (29).
> 8: Solve the combinatorial optimization in (32) or (34) to obtain $\{\hat{\boldsymbol{\Lambda}}, \hat{\boldsymbol{\Phi}}\}$
> 9: Estimate $\hat{\mathbf{h}} = [\hat{\mu}_{a_1} \; \hat{\mu}_{a_2} \ldots \; \hat{\mu}_{a_K}]$ by using (31) for a_k, $k = 1, 2, \ldots, K$, given in (42).
> 10: Estimate r_k and θ_k by employing (43) and (44).

---

estimation is summarized in Algorithm 1, where T_{EM} denotes the number of iterations of the EM algorithm.[5]

VI. MULTIPLE ANTENNAS RECEIVER

In this section, we extend the derived maximum likelihood cost function and the proposed EM-based joint range and PO estimators to the case of multiple receive antennas.

A. Maximum Likelihood and EM Estimators

We consider N_{r} single antenna receivers where we assume that the distance between the receive antenna elements is more than half a wavelength. Under this assumption, the coupling effect can be neglected and spatially uncorrelated Gaussian noise can be considered. We propose a time-domain estimator and does not consider the directivity of the multiple receive antennas in contrast to an antenna array because of the random phase of each receiver. It should be mentioned that an antenna array is a set of multiple connected antennas which work together as a single antenna to transmit or receive radio waves. However, we consider independent single antenna receivers that take the advantage of combining gain.

With the assumption that the time delay between receive antennas is negligible, and the path loss between the kth drone and ℓth receive antenna is the same for all receive antennas, i.e, $L_{\ell,k} = L_k$, $k = 1, 2, \ldots, K$, $\ell = 1, 2, \ldots, N_{\mathrm{r}}$, the received complex baseband signal at the multiple-receive antennas can be expressed as

$$\mathbf{Y} = \mathbf{HX} + \mathbf{W}, \qquad (45)$$

where $\mathbf{X} \triangleq [\mathbf{x}_1 \; \mathbf{x}_2 \; \cdots \; \mathbf{x}_K]^T \in \mathbb{C}^{K \times (N+1)}$, $\mathbf{Y} \triangleq [\mathbf{y}_0 \; \mathbf{y}_1 \cdots \; \mathbf{y}_N] \in \mathbb{C}^{N_{\mathrm{r}} \times (N+1)}$, $\mathbf{x}_k$ is given by (6), and $\mathbf{y}_n \triangleq [y_{1,n} \; y_{2,n} \; \cdots \; y_{N_{\mathrm{r}},n}]^T$ denotes the received vector

at time index n. In (45), the matrices $\mathbf{H} \in \mathbb{C}^{N_{\mathrm{r}} \times K}$ and $\mathbf{W} \in \mathbb{C}^{N_{\mathrm{r}} \times (N+1)}$ are given as

$$\mathbf{H} = \begin{bmatrix} \mathbf{h}_1^T \\ \mathbf{h}_2^T \\ \vdots \\ \mathbf{h}_{N_{\mathrm{r}}}^T \end{bmatrix}, \qquad \mathbf{W} = \begin{bmatrix} \mathbf{w}_1^T \\ \mathbf{w}_2^T \\ \vdots \\ \mathbf{w}_{N_{\mathrm{r}}}^T \end{bmatrix}, \qquad (46)$$

where

$$\mathbf{h}_\ell \triangleq \begin{bmatrix} h_{\ell,1} \; h_{\ell,2} \; \ldots \; h_{\ell,K} \end{bmatrix}^T$$
$$= \begin{bmatrix} \beta_1 \exp(j\theta_{\ell,1}) \; \ldots \; \beta_N \exp(j\theta_{\ell,K}) \end{bmatrix}^T, \qquad (47)$$

$\beta_k = \beta_{\ell,k} = \sqrt{P_k L_k}$, $\mathbf{w}_\ell \triangleq [w_{\ell,0} \; w_{\ell,1} \; \ldots \; w_{\ell,N}]^T$ with $w_{\ell,n} \sim \mathcal{CN}(0, \sigma_{\mathrm{w}}^2)$ the complex Gaussian noise at the ℓth receive antenna at time index n. As seen, while $\beta_{1,k} = \beta_{2,k} = \cdots = \beta_{N_{\mathrm{r}},k} = \beta_k$, the phases $\theta_{1,k}, \theta_{2,k}, \ldots, \theta_{N_{\mathrm{r}},k}$ are independent random values in $[0 \; 2\pi)$.

The joint PDF of the elements of $\mathbf{Y}$ is given by

$$f_{\mathbf{Y}}\left(\mathbf{Y}; p, \boldsymbol{\beta}, \boldsymbol{\Theta}, \sigma_{\mathrm{w}}^2\right) = \prod_{\ell=1}^{N_{\mathrm{r}}} \prod_{n=0}^{N} f_Y\left(y_{\ell,n}; p, \boldsymbol{\beta}, \boldsymbol{\theta}_\ell, \sigma_{\mathrm{w}}^2\right), \quad (48)$$

where $\boldsymbol{\beta} \triangleq [\beta_1 \; \beta_2 \; \ldots \; \beta_K]^T$, $\boldsymbol{\Theta} \triangleq \begin{bmatrix} \boldsymbol{\theta}_1^T \; \boldsymbol{\theta}_2^T \; \ldots \; \boldsymbol{\theta}_{N_{\mathrm{r}}}^T \end{bmatrix}^T$, $\boldsymbol{\theta}_\ell \triangleq \begin{bmatrix} \theta_{\ell,1} \; \theta_{\ell,2} \; \ldots \; \theta_{\ell,K} \end{bmatrix}^T$, and $f_Y(y; p, \boldsymbol{\beta}, \boldsymbol{\theta}, \sigma_{\mathrm{w}}^2)$ is given in (14). We can easily write the direct MLE of the parameter vector $\boldsymbol{\beta}$ and $\boldsymbol{\Theta}$ as

$$\{\hat{\boldsymbol{\beta}}, \hat{\boldsymbol{\Theta}}\} = \arg\max_{\boldsymbol{\beta}, \boldsymbol{\Theta}} \sum_{\ell=1}^{N_{\mathrm{r}}} \sum_{n=0}^{N} \ln f_Y\left(y_{\ell,n}; p, \boldsymbol{\beta}, \boldsymbol{\theta}_\ell, \sigma_{\mathrm{w}}^2\right). \quad (49)$$

Solving the maximization problem in (49) is not straightforward. Hence, the direct MLE cannot be obtained. However, indirect estimation can be obtained by estimating the modes of the GM similar to the single receive antenna.

Analogous to the single receive antenna scenario, we can employ the EM algorithm for estimating the modes of the GM. For multiple receive antennas, the EM algorithm defines an identical latent random vector $\mathbf{u} \triangleq [u_0 \; u_1 \; \ldots \; u_N]^T$ for all receive antennas. This random vector determines the GM component from which the observation originates, i.e.,

$$f_Y\left(y_{\ell,n}|u_n = a; p, \boldsymbol{\beta}, \boldsymbol{\theta}_\ell, \sigma_{\mathrm{w}}^2\right) \sim \mathcal{CN}\left(y_{\ell,n}; \mu_{\ell,a}, \sigma_{\mathrm{w}}^2\right), \quad (50)$$

where $n = 0, 1, \ldots, N$, $\ell = 1, 2, \ldots, N_{\mathrm{r}}$, $a = 0, 1, \ldots, 2^K - 1$, $\mu_{\ell,a} \triangleq \sum_{k=1}^{K}(1 - b_k)h_{\ell,k} = \sum_{k=1}^{K}(1 - b_k)\beta_k \exp(j\theta_{\ell,k})$, $a = (b_K, b_{K-1}, \ldots, b_1)_2$, $b_i \in \{0, 1\}$, and $P_U(u_n = a) = \xi_a$.

The EM algorithm iteratively maximizes the expected value of the complete-data log-likelihood function to estimate the vector $\boldsymbol{\Gamma} \triangleq [\boldsymbol{\eta}_1^T \; \boldsymbol{\eta}_2^T \; \ldots \; \boldsymbol{\eta}_{N_{\mathrm{r}}}^T]^T$ as

$$\boldsymbol{\Gamma}^{(t+1)} = \arg\max_{\boldsymbol{\Gamma}} C\left(\boldsymbol{\Gamma}|\boldsymbol{\Gamma}^{(t)}\right), \qquad (51)$$

where the vector $\boldsymbol{\eta}_\ell \triangleq [\eta_{\ell,0} \; \eta_{\ell,1} \; \ldots \; \eta_{\ell,2^K-1}]^T$ denotes the 2^K modes of the 2D GM at the ℓth receive antenna, $\boldsymbol{\Gamma}^{(0)}$ is the initialization vector,

$$C\left(\boldsymbol{\Gamma}|\boldsymbol{\Gamma}^{(t)}\right) = \mathbb{E}_{\mathbf{U}|\mathbf{Y};\boldsymbol{\Gamma}^{(t)}}\left\{ \ln f_{\mathbf{Y},\mathbf{U}}\left(\mathbf{Y}, \mathbf{u}; p, \boldsymbol{\Gamma}, \sigma_{\mathrm{w}}^2\right) \right\}$$

---

[5]The pseudocode has been written for the reordering methods in (32) and (34). Similar pseudocode can be written for other reordering estimation methods.

ADS-B parameters for the simulation	
$P_{\mathrm{t}} = 51$ dBm	ADS-B transmit power
$f_{\mathrm{c}} = 1090$ MHz	Carrier frequency of the ADS-B system
$B_3 = 1.3$ MHz	3 dB bandwidth of the transmit ADS-B signal
$B_{20} = 7$ MHz	20 dB bandwidth of the transmit ADS-B signal
$B_{40} = 23$ MHz	40 dB bandwidth of the transmit ADS-B signal
$B_{60} = 78$ MHz	60 dB bandwidth of the transmit ADS-B signal
$T_{\mathrm{r}} = 0.01\mu s$	Rise time of the ADS-B trapezoidal transmit pulse
$T_{\mathrm{d}} = 0.01\mu s$	Decay time of the ADS-B trapezoidal transmit pulse
$T = 0.48\mu s$	Time of the ADS-B trapezoidal transmit pulse

$$= \sum_{\ell=1}^{N_{\mathrm{r}}} \sum_{n=0}^{N} \sum_{a=0}^{2^K-1} \delta_{a,n}^{(t)} \left(\ln \frac{\xi_a}{\pi\sigma_{\mathrm{w}}^2} - \frac{|y_{\ell,n} - \eta_{\ell,n}|^2}{\sigma_{\mathrm{w}}^2} \right), \quad (52)$$

$$\delta_{a,n}^{(t)} = P_{U|\boldsymbol{Y}}\left(u_n = a | \mathbf{y}_n; p, \boldsymbol{\Gamma}^{(t)}, \sigma_{\mathrm{w}}^2\right)$$

$$= \frac{P_U(u_n = a) f_{\boldsymbol{Y}|U}\left(\mathbf{y}_n | u_n = a; p, \boldsymbol{\Gamma}^{(t)}, \sigma_{\mathrm{w}}^2\right)}{\sum_{a=0}^{2^K-1} f_{\boldsymbol{Y},U}\left(\mathbf{y}_n, u_n = a; p, \boldsymbol{\Gamma}^{(t)}, \sigma_{\mathrm{w}}^2\right)}$$

$$= \frac{\xi_a \prod_{\ell=1}^{N_{\mathrm{r}}} \mathcal{CN}\left(y_{\ell,n}; \eta_{\ell,a}^{(t)}, \sigma_{\mathrm{w}}^2\right)}{\sum_{a=0}^{2^K-1} \xi_a \prod_{\ell=1}^{N_{\mathrm{r}}} \mathcal{CN}(y_{\ell,n}; \eta_{\ell,a}^{(t)}, \sigma_{\mathrm{w}}^2)}, \quad (53)$$

and the joint complete-data likelihood function is given by

$$f_{\boldsymbol{Y},\boldsymbol{U}}(\boldsymbol{Y}, \mathbf{u}; p, \boldsymbol{\Gamma}, \sigma_{\mathrm{w}}^2)$$

$$= \prod_{\ell=1}^{N_{\mathrm{r}}} \prod_{n=0}^{N} \prod_{a=0}^{2^K-1} \left(\xi_a \mathcal{CN}\left(y_{\ell,n}; \mu_{\ell,a}, \sigma_{\mathrm{w}}^2\right)\right)^{\mathbb{I}\{u_n=a\}}. \quad (54)$$

By solving the maximization problem in (51), the elements of $\boldsymbol{\eta}^{(t+1)}$ are iteratively updated as follows

$$\eta_{\ell,a}^{(t+1)} = \frac{\sum_{n=0}^{N} \delta_{a,n}^{(t)} y_{\ell,n}}{\sum_{n=0}^{N} \delta_{a,n}^{(t)}}. \quad (55)$$

The convergence condition for the EM algorithm is $\|\boldsymbol{\Upsilon}^{(t+1)} - \boldsymbol{\Upsilon}^{(t)}\| < \epsilon$, where ϵ is a preset threshold. We denote $\hat{\eta}_{\ell,a} = \eta_{\ell,a}^{(t+1)}$ when the EM algorithm converges at the $(t+1)$th iteration.

While the EM algorithm estimates $N_{\mathrm{r}} 2^K$ parameters, only $N_{\mathrm{r}} K$ parameters are used for joint ranging and PO estimation of K drones. These $N_{\mathrm{r}} K$ modes are $\mu_{\ell,a_1}, \mu_{\ell,a_2}, \ldots, \mu_{\ell,a_K}$, where a_k is defined in (42). After the EM convergence, each receive antenna independently applies estimation mapping as explained in Section V. Let $\hat{\mu}_{\ell,a_1}, \hat{\mu}_{\ell,a_2}, \ldots, \hat{\mu}_{\ell,a_K}$ denote the estimated and reordered modes at the ℓth receive antenna. By averaging, then we can write

$$|\hat{\mu}_{a_k}| = \frac{1}{N_{\mathrm{r}}} \sum_{\ell=1}^{N_{\mathrm{r}}} |\hat{\mu}_{\ell,a_k}| \propto \frac{1}{\hat{r}_k}, \quad (56)$$

where $k = 1, 2, \ldots, K$. By substituting (56) into (43), we can estimate the range of the kth drone. The PO for each drone-receive antenna is obtained by replacing $\hat{\mu}_{\ell,a_1}, \hat{\mu}_{\ell,a_2}, \ldots, \hat{\mu}_{\ell,a_K}$, $\ell = 1, 2, \ldots, N_{\mathrm{r}}$ into (44).

It should be mentioned that the EM algorithm can also be implemented independently at each receive antennas. Then, after
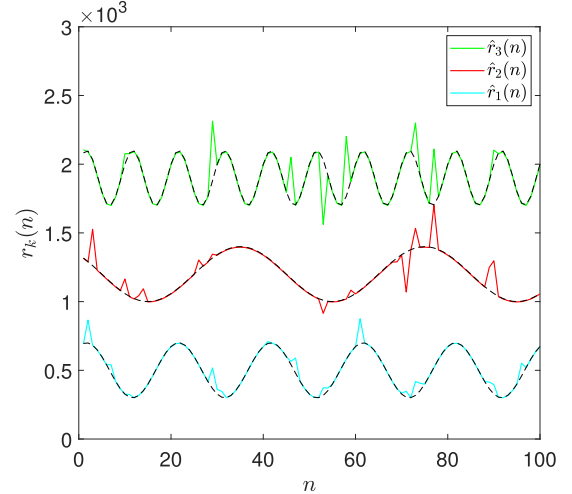

Fig. 6. Range tracking by the proposed EM-based estimator for $K = 3$ drones. The dashed and solid lines denote the true and estimated range, respectively.

reordering estimation, the ranges are obtained by averaging. This results in a lower complexity solution.

B. Outlier Detection

For multiple receive antennas at the receiver, it is possible that one or multiple outliers appear in the estimated sequence $|\hat{\mu}_{\ell,a_1}|, |\hat{\mu}_{\ell,a_1}|, \ldots, |\hat{\mu}_{\ell,a_K}|$, where a_k is given in (42). These outliers can increase the estimation error of $|\hat{\mu}_{a_k}|$ in (56) that is used for range estimation. To remove the effect of outliers, we can use outlier detection algorithms, such as the median absolute deviation (MAD) [33]. In this case, the averaging is performed over the receive antennas without outliers. This results in a significant performance improvement in range estimation.

C. Computational Complexity Analysis

In each iteration of the EM algorithm, we evaluate $N_{\mathrm{r}} 2^K$ Gaussian densities for $N + 1$ observation points in the E-step in (52), and its computational cost scales as $O(N_{\mathrm{r}} N 2^K)$. The computational cost of the M-step in (55) per iteration also scales as $O(N_{\mathrm{r}} N 2^K)$. The complexity of the k-means++ initialization is $O(N_{\mathrm{r}} N 2^K)$. The number of combinatorial search for reordering estimation via the LS and the proposed linear/non-linear combinations minimization is $(2^K - 1)!$ and $C_Q^{2^K-1}$, $Q = 1, 2, \ldots, 2^K - 1$, (depending on the selected linear/non-linear combinations), respectively. Hence, for $K \geq 4$, the method of linear/non-liner combinations minimization is more computationally efficient for reordering estimation.

VII. SIMULATION

In this section, we examine the performance of the proposed EM-based joint range and PO estimator through several simulation experiments to confirm the effectiveness of the proposed algorithm.
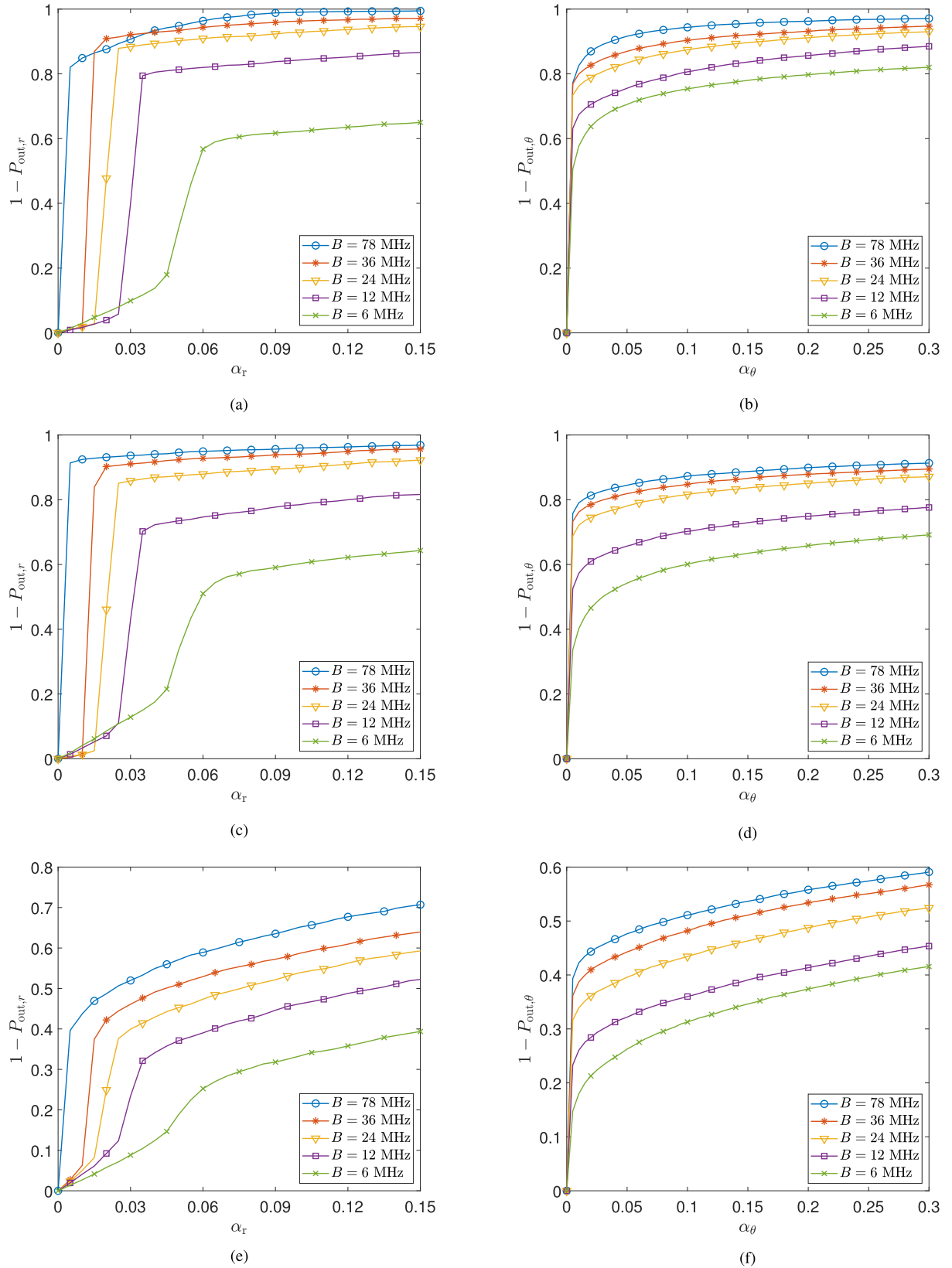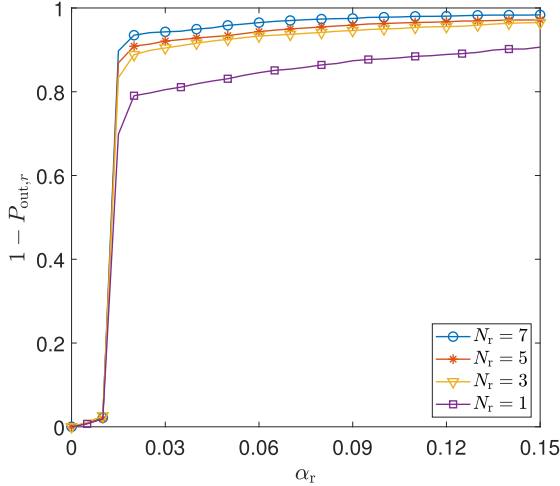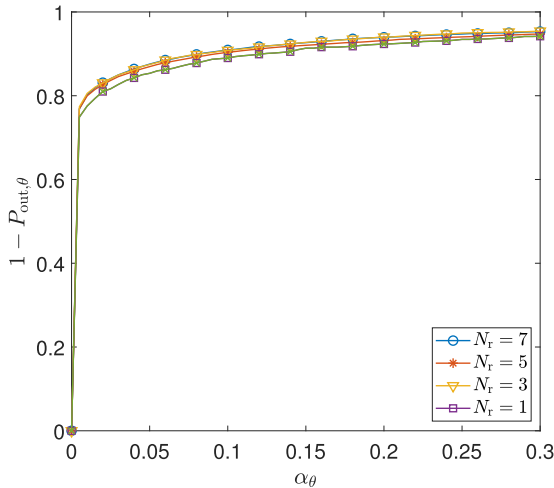
Fig. 7. Performance of the proposed joint EM-based estimator for different number of drones, K, $P_1 = P_2 = \ldots = P_K = 51$ dBm, $r_1, r_2, \ldots r_K \in \mathcal{U}_c[1, 10]$ Km, and $N_r = 5$. (a) Range estimation for $K = 2$ drones. (b) PO estimation for $K = 2$ drones. (c) Range estimation for $K = 3$ drones. (d) PO estimation for $K = 3$ drones. (e) Range estimation for $K = 4$ drones. (f) PO estimation for $K = 4$ drones.
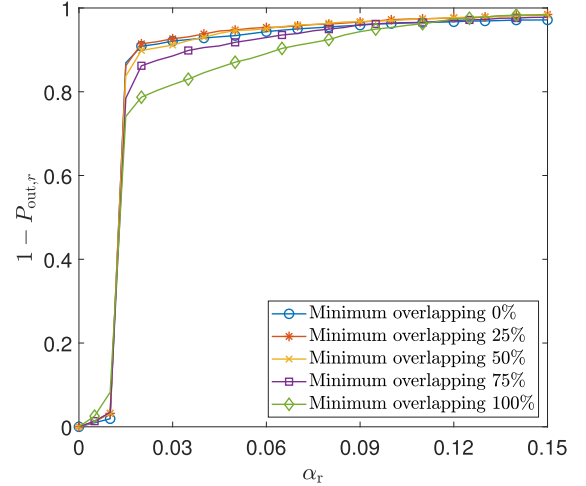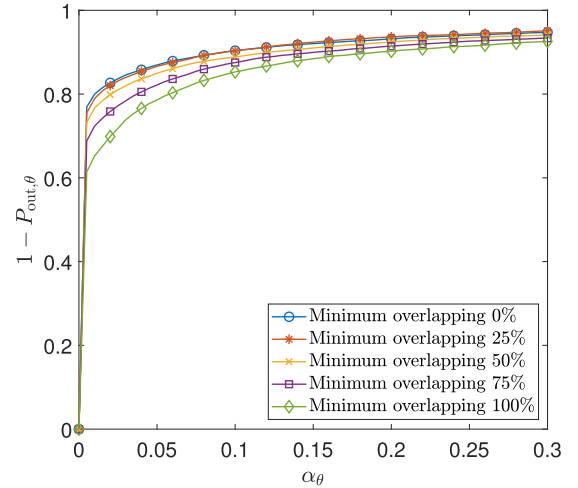
Fig. 8. Effect of the number of receive antennas, N_r, on the performance of the proposed EM-based joint estimator for $K = 2$ drones, $P_1 = P_2 = 51$ dBm, $r_1, r_2 \in \mathcal{U}_c[1, 10]$ Km, and $\theta_{1,1}, \theta_{1,2}, \theta_{2,1}, \theta_{2,2}, \in \mathcal{U}_c[-\pi, \pi)$. (a) The effect of N_r on range estimation. (b) The effect of N_r on PO estimation.

Fig. 9. Effect of the minimum overlapping percentage on the performance of the proposed EM-based joint estimator for $K = 2$ drones, $P_1 = P_2 = 51$ dBm, $r_1, r_2 \in \mathcal{U}_c[1, 10]$ Km, $\theta_{1,1}, \theta_{1,2}, \theta_{2,1}, \theta_{2,2}, \in \mathcal{U}_c[-\pi, \pi)$, and $N_r = 5$. (a) The effect of minimum overlapping on range estimation. (b) The effect of minimum overlapping on PO estimation.

A. Simulation Setup

Unless otherwise mentioned, we considered K drones with ranges $r_1, r_2, \ldots, r_K \in \mathcal{U}_c[1, 10]$ Km. The azimuth and elevation angles of the drones are assumed to be $\phi_1, \phi_2, \ldots, \phi_K \in \mathcal{U}_c[-\pi, \pi)$ and $\psi_1, \psi_2, \ldots, \psi_K \in \mathcal{U}_c[0, \pi/2]$, respectively. We considered free space path loss model in (2) and $\lambda_c \approx 0.2752$ m for ADS-B systems. The number of receive antennas was set to $N_r = 5$. For ADS-B message period of $T_P = 240\mu$s, the discrete time delay of each drone for each ADS-B packet transmission is assumed to be modeled by a discrete i.i.d. random variable with uniform distribution as $m_1, m_2, \ldots, m_K \in \mathcal{U}_d[0, M]$, where $M \triangleq \lfloor 2BT_p \rfloor$ with B as the bandwidth of the square-root-raised-cosine (SRRC) receive baseband filter $h(t)$ with roll-off factor $\beta = 0.9$ and group delay $\tau_{gr} = 47.25\mu$s. Without loss of generality, we consider that $E_h \triangleq \int_{-\infty}^{+\infty} |h(t)|^2 dt =$

$\int_{-B}^{+B} |H(f)|^2 df = 1$, where $H(f)$ is the frequency response of the receive filter.

We also assumed that the PO between the kth drone and the ℓth receive antenna is modeled by a continuous i.i.d. random variable with uniform distribution as $\theta_{\ell,k} \in \mathcal{U}_c[0, 2\pi)$, $k = 1, 2, \ldots, K$, $\ell = 1, 2, \ldots, N_r$. Without loss of generality, we considered that $P_1 = P_2 = \cdots = P_K = 51$ dBm [34], and the noise power in dBm at each receive antennas is considered to be $\sigma_w^2 = 10 \log_{10}((N_0 E_h)/10^{-3}) = -174$. The parameters of the ADS-B PPM waveform for the simulation are summarized in Table I.

The performance of the proposed EM-based joint range and PO estimator was evaluated in terms of $1 - P_{out,r}$ and $1 - P_{out,\theta}$ where

$$P_{out,r} \triangleq \frac{1}{K} \sum_{k=1}^{K} \mathbb{P} \left\{ \frac{|\hat{r}_k - r_k|}{r_k} > \alpha_r \right\},$$
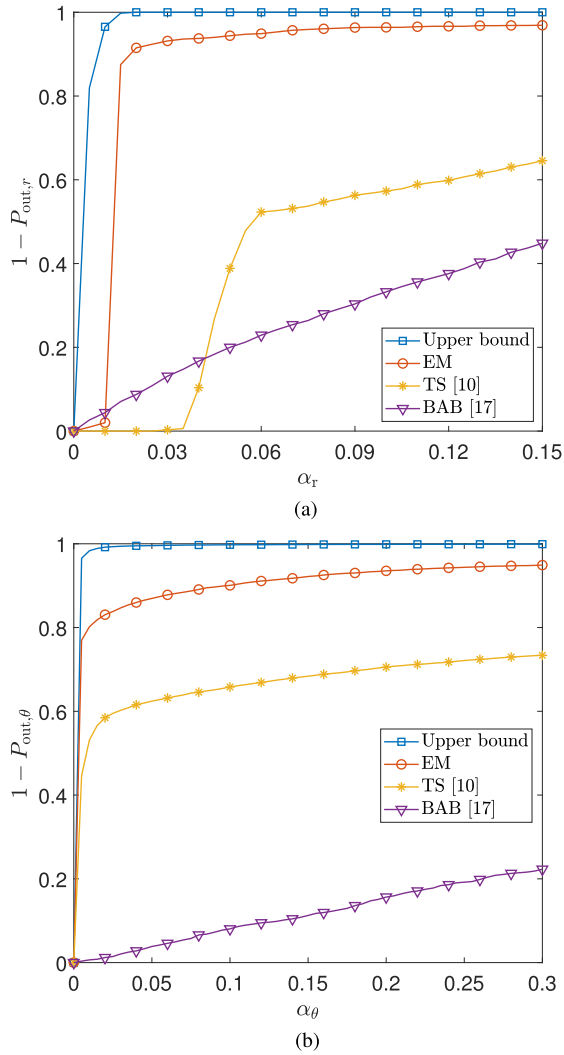
Fig. 10. Performance comparison of the proposed EM-based joint estimator for $K = 2$ drones, $P_1 = P_2 = 51$ dBm, $r_1, r_2 \in \mathcal{U}_c[1, 10]$ Km, $\theta_{1,1}, \theta_{1,2}, \theta_{2,1}, \theta_{2,2}, \in \mathcal{U}_c[-\pi, \pi)$, and $N_r = 5$. (a) Performance comparison for range estimation. (b) Performance comparison for PO estimation.

and

$$P_{\text{out},\theta} \triangleq \frac{1}{KN_r} \sum_{\ell=1}^{N_r} \sum_{k=1}^{K} \mathbb{P}\left\{ \frac{|\hat{\theta}_{\ell,k} - \theta_{\ell,k}|}{\theta_{\ell,k}} > \alpha_\theta \right\},$$

with $\hat{r}_k$ as the estimated range of the kth drone and $\hat{\theta}_{\ell,k}$ as the PO of the kth drone at the ℓth receive antenna. The EM algorithm was run with 100 different random initial values by using the k-means++ initialization, and we considered the minimization problem in (32) for $K = 2, 3$ and (38) for $K = 4$ for reordering estimation. The number of Monte Carlo runs is 10^4.

B. Simulation Results

To illustrate the performance of the proposed EM-based joint estimator over time, we show range tracking for $K = 3$ drones with transmit power $P_1 = P_2 = P_3 = 51$ dBm in Fig. 6. It is considered that the ADS-B packets overlap. The range, delay, and PO variations versus index of the ADS-B packet, n, for the three

drones are modeled as $r_1(n) = 500 + 200\cos(0.1\pi n + \pi/3)$, $r_2(n) = 1200 + 200\cos(0.05\pi n + 2\pi/4)$, $r_3(n) = 1900 + 200\cos(0.2\pi n + \pi/6)$, $m_k(n) \in \mathcal{U}_d[0, 17280]$, $\theta_{\ell,k}(n) \in \mathcal{U}_c[0, 2\pi)$ for $\ell = 1, 2, \ldots, 5$, $k = 1, 2, 3$, $n = 1, 2, \ldots, 100$, and $B = 36$ MHz. We consider that $\mathbb{E}\{\theta_{\ell_1,k_1}(n_1)\theta_{\ell_2,k_2}(n_2)\} = (\pi^2/3)\delta[\ell_1 - \ell_2]\delta[k_1 - k_2]\delta[n_1 - n_2]$. As seen, the proposed EM-based estimator can accurately track the range of $K = 3$ drones. While the estimation error for the closest drone to the receiver is lower, i.e., $\mathbb{E}\{|r_1 - \hat{r}_1|\}^2 < \mathbb{E}\{|r_2 - \hat{r}_2|\}^2 < \mathbb{E}\{|r_3 - \hat{r}_3|\}^2$, $1 - P_{\text{out},r}$ is almost the same for all drones.

Fig. 7 illustrates $1 - P_{\text{out},r}$ and $1 - P_{\text{out},\theta}$ of the proposed EM-based joint estimator versus α_r and α_θ for different number of drones $K = 2, 3, 4$ and different values of receive filter bandwidth B. As seen, by increasing B, the performance of the EM-based joint estimator improves because sharp pulses are received at the receiver, and thus; the approximation error of received signal model in (1) reduces. Moreover, as expected, the larger number of drones, higher estimation error. The reason is that the number of GM components to be estimated by the EM algorithm exponentially increases with K, i.e., 2^K; however, the number of observation samples remains fixed.

Fig. 8 shows the effect of the number of receive antennas on the range and PO estimation versus α_r and α_θ for $K = 2$ drones, $P_1 = P_2 = 51$ dBm, and $B = 36$ MHz. As seen, the larger number of receive antennas, N_r, higher $1 - P_{\text{out},r}$. Also, the rate of performance improvement decreases as the number of receive antennas increases. As expected, increasing the number of receive antennas does not affect $1 - P_{\text{out},\theta}$ because spatial diversity is not employed for the estimation of the KN_r independent POs. However, the range estimation takes the advantage of spatial diversity. The interesting property of the proposed algorithm is that it can jointly estimate the range and PO of multiple drones/aircrafts with a single receive antenna. With a single receive antenna, the range accuracy of $\alpha_r = 0.03$ is archived for 80% of the time.

Fig. 9 illustrates the performance of the proposed EM-based joint estimator for different minimum overlapping percentage of the ADS-B packets for $K = 2$ drones/aircrafts, $N_r = 5$ receive antennas, and $B = 36$ MHz. As expected, the lower minimum overlapping percentage, more accurate ranging and PO estimation because interference decreases.

In Fig. 10, we compare the performance of the proposed EM-based joint estimator with the time segmentation (TS) and the blind adaptive beamforming (BAB) ADS-B packet separation methods in [10] and [17] for $K = 2$ drones/aircrafts, $N_r = 5$ receive antennas, and $B = 36$ MHz. The TS and BAB methods first separate the ADS-B packets. Then, by using the separated packets, they can estimate the range and PO of the drones. As seen, our proposed method outperforms the TS and the BAB methods because it employs all the observation samples including the overlapping snapshot for ranging and PO estimation; however, the TS and the BAB methods rely on the non-overlapping snapshot for ADS-B packet recovery. Hence, as the delay between the reception of two ADS-B packets decreases, their performance degrades. It should be mentioned that while the TS and the BAB methods can be used to estimate the range of maximum $K = 2$ drones; our proposed method

can estimate the range of $K > 1$ drones with a single receive antenna. In Fig. 10, we also show performance of the efficient estimator[6] [32]. For the efficient estimator, the transmit symbols and delay of the drones/aircrafts are assumed to be known a priori at the receiver. As seen, there is a small gap between the performance of the proposed estimator and the efficient estimator while the transmit symbols and delay of the drones/aircraft are unknown to the EM-based estimator.

VIII. CONCLUSION

In this article, we showed that the lost ADS-B packets due to packet collisions can be employed to jointly estimate range and PO of multiple drones/aircrafts in the airspace. This enables drones to maintain safe operation distance in the congested airspace, where ADS-B packet decoding is impossible due to packet collisions. To achieve this, we derived the maximum likelihood and EM-based joint range and PO estimators using an approximate PDF obtained by KLD minimization. The proposed estimators consider uncoordinated and asynchronous ADS-B packet transmission. For joint range and PO estimation, a priori knowledge or estimation of the drones' time delay is not required. Simulation results showed that the EM-based joint estimator can estimate the range of multiple drones/aircrafts with a single receive antenna. Performance improvement by employing multiple receive antennas is obtained.

APPENDIX A
PROOF OF THEOREM 1

The vector $\mathbf{x}_k$ given hypothesis H_m^k in (7) is composed of 4 ones and 12 zeros in $\mathbf{s}$. The number of zeros and ones in the data field $\mathbf{d}_k$ is 112 due to Manchester encoding. Moreover, M zeros are added irrespective to the hypothesis H_m^k because of the maximum integer delay. Hence, the total number of zeros and ones in $\mathbf{x}_k$ are $M + 124$ and 116, respectively.

Let $\mathcal{X}_m^k$ denote all possible vector for $\mathbf{x}_k$ given hypothesis H_m^k. The cardinality of $\mathcal{X}_m^k$, i.e., $|\mathcal{X}_m^k| = 2^{112}$ since the randomness in $\mathbf{x}_k$ because of the data field $\mathbf{d}_k$ results in 2^{112} different Manchester encoded sequences. Thus; the joint PMF of $x_{k,0}, x_{k,1}, \ldots, x_{k,N}$ is given by

$$f(\mathbf{x}_k) = f\big(x_{k,0}, x_{k,1}, \ldots, x_{k,N}|H_m^k\big)$$
$$= \begin{cases} \frac{1}{2^{112}} & \mathbf{x}_k \in \mathcal{X}_m^k, \\ 0 & \mathbf{x}_k \notin \mathcal{X}_m^k. \end{cases} \tag{57}$$

Let us consider the following approximation for the joint PMF in (57).

$$f(\mathbf{x}_k) = f\big(x_{k,0}, x_{k,1}, \ldots, x_{k,N}|H_m^k\big)$$
$$\approx \prod_{n=0}^{N} g(x_{k,n}|H_m^k) \tag{58}$$

[6]An efficient estimator is an unbiased estimator that attains the Cramer-Rao Lower Bound (CRLB) [35].

The KLD for f and g in (58) is given by

$$D(f\|g) = \sum_{\mathcal{X}_m^k} \left[f\big(x_{k,0}, x_{k,1}, \ldots, x_{k,N}|H_m^k\big) \right.$$
$$\left. \times \ln \frac{f\big(x_{k,0}, x_{k,1}, \ldots, x_{k,N}|H_m^k\big)}{\prod_{n=0}^{N} g(x_{k,n}|H_m^k)} \right]. \tag{59}$$

Because $x_{k,n} \in \{0, 1\}$ for $n = 0, 1, \ldots, N$, the KLD is minimized for Bernoulli distribution. The PMF of Bernoulli distribution is expressed as

$$g(i|H_m^k) = \begin{cases} p & \text{if } i = 0, \\ 1 - p & \text{if } i = 1, \end{cases} \tag{60}$$

where $p \in [0, 1]$.

By substituting the PMF in (57) and (60) into (59), and by using the fact that $\sum_{n=0}^{N} x_{k,n} = 116$ for $\mathbf{x}_k \in \mathcal{X}_m^k$, we can write the KLD in (59) as

$$D(f\|g) = \frac{1}{2^{112}} \sum_{\mathcal{X}_m^k} \ln \left[\frac{1}{2^{212}p^{M+124}(1-p)^{116}} \right]$$
$$= -\ln \left[2^{212}p^{M+124}(1-p)^{116} \right]. \tag{61}$$

To obtain p, we need to minimize $D(f\|g)$. Because $\ln(\cdot)$ is a monotonically increasing function, $D(f\|g)$ is minimized when $p^{M+124}(1-p)^{116}, p \in [0, 1]$, is maximized. By taking the derivative with respect to p and setting it to zero, we obtain

$$\frac{\mathrm{d}\big(p^{M+124}(1-p)^{116}\big)}{\mathrm{d}p} = (M+124)p^{M+123}(1-p)^{116}$$
$$- 116(1-p)^{115}p^{M+124} = 0. \tag{62}$$

By solving (62), we obtain (9).

APPENDIX B
PROOF OF THE PDF OF $G = \sum_{k=1}^{K} Z_k$

Let us consider $G = \sum_{k=1}^{K} Z_k$. Since Z_k, $k = 1, 2, \ldots, K$, are independent random variables, the PDF of G is given by

$$f_G(g; p, \mathbf{h}) = f_{Z_1}\big(z; p, h_1\big) * f_{Z_2}\big(z; p, h_2\big)$$
$$* \ldots * f_{Z_K}\big(z; p, h_K\big), \tag{63}$$

where $z \triangleq z_{\mathrm{r}} + iz_{\mathrm{I}} \in \mathbb{C}$, $\mathbf{h} \triangleq [h_1, h_2, \ldots, h_K]^T$, $h_k \triangleq (h_k)_{\mathrm{r}} + i(h_k)_{\mathrm{I}} \in \mathbb{C}$, and $f_{Z_k}\big(z; p, h_k\big)$ is given in (10). The two-dimensional Laplace transform of $f_{Z_k}\big(z; p, h_k\big)$ is expressed as

$$F_{Z_k}\big(s_1, s_2; p, h_k\big) = \int_{-\infty}^{+\infty} \int_{-\infty}^{+\infty} f_{Z_k}\big(z; p, h_k\big) e^{-s_1 z_{\mathrm{r}} - s_2 z_{\mathrm{I}}} \mathrm{d}z_{\mathrm{r}} \mathrm{d}z_{\mathrm{I}}$$
$$= \int_{-\infty}^{+\infty} \int_{-\infty}^{+\infty} p\delta(z_{\mathrm{r}})\delta(z_{\mathrm{I}}) e^{-s_1 z_{\mathrm{r}} - s_2 z_{\mathrm{I}}} \mathrm{d}z_{\mathrm{r}} \mathrm{d}z_{\mathrm{I}}$$
$$+ \int_{-\infty}^{+\infty} \int_{-\infty}^{+\infty} (1-p)\delta(z_{\mathrm{r}} - (h_k)_{\mathrm{r}})\delta(z_{\mathrm{I}} - (h_k)_{\mathrm{I}}) e^{-s_1 z_{\mathrm{r}} - s_2 z_{\mathrm{I}}} \mathrm{d}z_{\mathrm{r}} \mathrm{d}z_{\mathrm{I}}$$
$$= p + (1-p)e^{-((h_k)_{\mathrm{r}} s_1 + (h_k)_{\mathrm{I}} s_2)}.$$

Using the fact that the linear convolution is equivalent to multiplication in the Laplace domain, we can write

$$F_G\big(s_1, s_2; p, \mathbf{h}\big) = \prod_{k=1}^{K} F_{Z_k}\big(s_1, s_2; p, h_k\big)$$

$$= \prod_{k=1}^{K} \left[p + (1-p)e^{-((h_k)_{\mathrm{r}} s_1 + (h_k)_{\mathrm{I}} s_2)} \right], \tag{64}$$

where $F_G\big(s_1, s_2; p, \mathbf{h}\big)$ denotes the two-dimensional Laplace transform of $f_G(g; p, \mathbf{h})$. Let us consider the multi-binomial theorem as follows [28]

$$\prod_{i=1}^{d}(a_i + b_i)^{n_i}$$

$$= \sum_{v_1=0}^{n_1} \cdots \sum_{v_d=0}^{n_d} \binom{n_1}{v_1} a_1^{v_1} b_1^{n_1-v_1} \cdots \binom{n_d}{v_d} a_d^{v_d} b_d^{n_d-v_d}. \tag{65}$$

By substituting $a_i \triangleq p$, $b_i \triangleq (1-p)e^{-((h_i)_{\mathrm{r}} s_1 + (h_i)_{\mathrm{I}} s_2)}$, $d = K$, and $n_i = 1$, $i = 1, 2, \ldots, d$, into (65), we obtain

$$F_G\left(s_1, s_2; p, \mathbf{h}\right) = \sum_{v_1=0}^{1} \cdots \sum_{v_K=0}^{1} \left[p^{\sum_{k=1}^{K} v_k}(1-p)^{K-\sum_{k=1}^{K} v_k} \right.$$

$$\left. \times \exp\left[-\sum_{k=1}^{K}(1-v_k)((h_k)_{\mathrm{r}} s_1 + (h_k)_{\mathrm{I}} s_2) \right] \right]. \tag{66}$$

The two-dimensional inverse Laplace transform of the exponential term in (66) is given by

$$\mathcal{L}^{-1}\left\{ \exp\left[-\sum_{k=1}^{K}(1-v_k)((h_k)_{\mathrm{r}} s_1 + (h_k)_{\mathrm{I}} s_2) \right] \right\}$$

$$= \delta\left(s_{\mathrm{r}} - \sum_{k=1}^{K}(1-v_k)(h_k)_{\mathrm{r}} \right) \delta\left(s_{\mathrm{I}} - \sum_{k=1}^{K}(1-v_k)(h_k)_{\mathrm{I}} \right)$$

$$= \delta_{\mathrm{c}}\left(s - \sum_{k=1}^{K}(1-v_k) h_k \right), \tag{67}$$

where $s = s_{\mathrm{r}} + i s_{\mathrm{I}} \in \mathbb{C}$. By taking two-dimensional inverse Laplace transform from both sides of (66) and then employing (67), we obtain $f_G(g; p, \mathbf{h})$ as in (12).

APPENDIX C

For $K = 2$, we have

$$\boldsymbol{\mu} \triangleq \big[\mu_0\ \mu_1\ \mu_2\ \mu_3\big]^T$$

$$= \big[\beta_1 \exp(j\theta_1) + \beta_2 \exp(j\theta_2)\ \ \beta_2 \exp(j\theta_2)\ \ \beta_1 \exp(j\theta_1)\ \ 0\big]^T, \tag{68}$$

where $\beta_1 > \beta_2$, and for $K = 3$, we can write

$$\boldsymbol{\mu} \triangleq \big[\mu_0\ \mu_1\ \mu_2\ \mu_3\ \mu_4\ \mu_5\ \mu_6\ \mu_7\big]^T$$

$$= \big[\beta_1 \exp(j\theta_1) + \beta_2 \exp(j\theta_2) + \beta_3 \exp(j\theta_3)$$

$$\beta_2 \exp(j\theta_2) + \beta_3 \exp(j\theta_3)\ \ \beta_1 \exp(j\theta_1) + \beta_3 \exp(j\theta_3)$$

$$\beta_3 \exp(j\theta_3)\ \ \beta_1 \exp(j\theta_1) + \beta_2 \exp(j\theta_2)\ \ \beta_2 \exp(j\theta_2)$$

$$\beta_1 \exp(j\theta_1)\ \ 0\big]^T, \tag{69}$$

with $\beta_1 > \beta_2 > \beta_3$. For $K = 4$, we can write

$$\boldsymbol{\mu} \triangleq \big[\mu_0\ \mu_1\ \mu_2\ \mu_3\ \mu_4\ \mu_5\ \mu_6\ \mu_7\ \cdots\ \mu_{13}\ \mu_{14}\ \mu_{15}\big]^T$$

$$= \big[\beta_1 \exp(j\theta_1) + \beta_2 \exp(j\theta_2) + \beta_3 \exp(j\theta_3) + \beta_4 \exp(j\theta_4)$$

$$\beta_2 \exp(j\theta_2) + \beta_3 \exp(j\theta_3) + \beta_4 \exp(j\theta_4)$$

$$\beta_1 \exp(j\theta_1) + \beta_3 \exp(j\theta_3) + \beta_4 \exp(j\theta_4)$$

$$\beta_3 \exp(j\theta_3) + \beta_4 \exp(j\theta_4)$$

$$\beta_1 \exp(j\theta_1) + \beta_2 \exp(j\theta_2) + \beta_4 \exp(j\theta_4)$$

$$\beta_2 \exp(j\theta_2) + \beta_4 \exp(j\theta_4)$$

$$\beta_1 \exp(j\theta_1) + \beta_4 \exp(j\theta_4)\ \ \beta_4 \exp(j\theta_4)$$

$$\beta_1 \exp(j\theta_1) + \beta_2 \exp(j\theta_2) + \beta_3 \exp(j\theta_3)$$

$$\beta_2 \exp(j\theta_2) + \beta_3 \exp(j\theta_3)\ \ \beta_1 \exp(j\theta_1) + \beta_3 \exp(j\theta_3)$$

$$\beta_3 \exp(j\theta_3)\ \ \beta_1 \exp(j\theta_1) + \beta_2 \exp(j\theta_2)\ \ \beta_2 \exp(j\theta_2)$$

$$\beta_1 \exp(j\theta_1)\ \ 0\big]^T, \tag{70}$$

where $\beta_1 > \beta_2 > \beta_3 > \beta_4$.

REFERENCES

[1] M. Strohmeier, M. Schäfer, V. Lenders, and I. Martinovic, "Realities and challenges of nextgen air traffic management: The case of ADS-B," *IEEE Commun. Mag.*, vol. 52, no. 5, pp. 111–118, May 2014.

[2] E. Tohidi, A. Hariri, H. Behroozi, M. M. Nayebi, G. Leus, and A. P. Petropulu, "Compressed-domain detection and estimation for colocated MIMO radar," *IEEE Trans. Aerosp. Electron. Syst.*, vol. 56, no. 6, pp. 4504–4518, Dec. 2020.

[3] Y. Kim, J.-Y. Jo, and S. Lee, "ADS-B vulnerabilities and a security solution with a timestamp," *IEEE Aerosp. Electron. Syst. Mag.*, vol. 32, no. 11, pp. 52–61, Nov. 2017.

[4] P. Angelov, *Sense and Avoid in UAS: Research and Applications*. Hoboken, NJ, USA: Wiley, 2012.

[5] F. Minucci, E. Vinogradov, and S. Pollin, "Avoiding collisions at any (low) cost: ADS-B like position broadcast for UAVs," *IEEE Access*, vol. 8, pp. 121843–121857, 2020.

[6] E. Vinogradov, F. Minucci, and S. Pollin, "Wireless communication for safe UAVs: From long-range deconfliction to short-range collision avoidance," *IEEE Veh. Technol. Mag.*, vol. 15, no. 2, pp. 88–95, Jun. 2020.

[7] Z. Luo, C. Li, and L. Zhu, "A comprehensive survey on blind source separation for wireless adaptive processing: Principles, perspectives, challenges and new research directions," *IEEE Access*, vol. 6, pp. 66685–66708, 2018.

[8] G. Chabriel, M. Kleinsteuber, E. Moreau, H. Shen, P. Tichavsky, and A. Yeredor, "Joint matrices decompositions and blind source separation: A survey of methods, identification, and applications," *IEEE Signal Process. Mag.*, vol. 31, no. 3, pp. 34–43, May 2014.

[9] G. R. Naik and D. K. Kumar, "An overview of independent component analysis and its applications," *Informatica*, vol. 35, no. 1, pp. 63–82, 2011.

[10] K. Li, J. Kang, H. Ren, and Q. Wu, "A reliable separation algorithm of ADS-B signal based on time domain," *IEEE Access*, vol. 9, pp. 88019–88026, 2021.

[11] R. Schmidt, "Multiple emitter location and signal parameter estimation," *IEEE Trans. Antennas Propag.*, vol. 34, no. 3, pp. 276–280, Mar. 1986.

[12] R. Roy and T. Kailath, "ESPRIT-estimation of signal parameters via rotational invariance techniques," *IEEE Trans. Acoust., Speech, Signal Process.*, vol. 37, no. 7, pp. 984–995, Jul. 1989.

[13] L. Tzafri and A. J. Weiss, "High-resolution direct position determination using MVDR," *IEEE Trans. Wireless Commun.*, vol. 15, no. 9, pp. 6449–6461, Sep. 2016.

[14] N. Petrochilos and A.-J. van der Veen, "Algorithms to separate overlapping secondary surveillance radar replies," in *Proc. IEEE Int. Conf. Acoust., Speech, Signal Process.*, Montreal, Canada, May 2004, pp. 49–52.

[15] N. Petrochilos, G. Galati, L. Mené, and E. Piracci, "Separation of multiple secondary surveillance radar sources in a real environment by a novel projection algorithm," in *Proc. IEEE 5th Int. Symp. Signal Process. Inf. Technol.*, 2005, pp. 125–130.

[16] N. Petrochilos, G. Galati, and E. Piracci, "Separation of SSR signals by array processing in multilateration systems," *IEEE Trans. Aerosp. Electron. Syst.*, vol. 45, no. 3, pp. 965–982, Jul. 2009.

[17] W. Wang, R. Wu, and J. Liang, "ADS-B signal separation based on blind adaptive beamforming," *IEEE Trans. Veh. Technol.*, vol. 68, no. 7, pp. 6547–6556, Jul. 2019.

[18] N. Petrochilos and A.-J. van Der Veen, "Algebraic algorithms to separate overlapping secondary surveillance radar replies," *IEEE Trans. Signal Process.*, vol. 55, no. 7, pp. 3746–3759, Jul. 2007.

[19] Z. Zhang, "Optimization performance analysis of 1090ES ADS-B signal separation algorithm based on PCA and ICA," *Int. J. Performability Eng.*, vol. 14, no. 4, 2018, Art. no. 741.

[20] M. Leonardi and M. Maisano, "Degarbling technique for low cost ADS-B receivers," in *Proc. IEEE 5th Int. Workshop Metrol. Aerosp.*, 2019, pp. 65–69.

[21] L. Dan and C. Tao, "Single-antenna overlapped ADS-B signal self-detection and separation algorithm based on EMD," *J. Signal Process.*, vol. 35, no. 10, pp. 1680–1689, 2019.

[22] R. Wu, C. Wu, and W. Wang, "A method of overlapped ADS-B signal processing based on accumulation and classification," *J. Signal Process.*, vol. 33, no. 4, pp. 572–576, 2017.

[23] Y. Sunquan, C. Lihu, L. Songting, and L. Lanmin, "Separation of space-based ADS-B signals with single channel for small satellite," in *Proc. IEEE 3rd Int. Conf. Signal Image Process.*, 2018, pp. 315–321.

[24] Y. Bi and C. Li, "Multi-scale convolutional network for space-based ADS-B signal separation with single antenna," *Appl. Sci.*, vol. 12, no. 17, 2022, Art. no. 8816.

[25] W. Wang, J. Liu, and J. Liang, "Single antenna ADS-B overlapping signals separation based on deep learning," *Digit. Signal Process.*, vol. 132, 2022, Art. no. 103804.

[26] M. Shi, Y. Bar-Ness, and W. Su, "Adaptive estimation of the number of transmit antennas," in *Proc. IEEE Mil. Commun. Conf.*, 2007, pp. 1–5.

[27] M. Mohammadkarimi, E. Karami, O. A. Dobre, and M. Z. Win, "Number of transmit antennas detection using time-diversity of the fading channel," *IEEE Trans. Signal Process.*, vol. 65, no. 15, pp. 4031–4046, Aug. 2017.

[28] C. Morris, "Central limit theorems for multinomial sums," *Ann. Statist.*, vol. 3, pp. 165–188, Jan. 1975.

[29] G. J. McLachlan, S. X. Lee, and S. I. Rathnayake, "Finite mixture models," *Annu. Rev. Statist. Appl.*, vol. 6, pp. 355–378, 2019.

[30] S. Theodoridis, *Machine Learning: A Bayesian and Optimization Perspective*. Cambridge, MA, USA: Academic Press, 2015.

[31] T. K. Moon, "The expectation-maximization algorithm," *IEEE Signal Process. Mag.*, vol. 13, no. 6, pp. 47–60, Nov. 1996.

[32] S. M. Kay, *Fundamentals of Statistical Signal Processing: Estimation Theory*. Hoboken, NJ, USA: Prentice-Hall, 1993.

[33] V. Chandola, A. Banerjee, and V. Kumar, "Anomaly detection: A survey," *ACM Comput. Surv.*, vol. 41, 2009, Art. no. 15.

[34] M. Series, "Reception of automatic dependent surveillance broadcast via satellite and compatibility studies with incumbent systems in the frequency band 1 087.7-1 092.3 MHz," Int. Telecommun. Union, Geneva, Switzerland, Tech. Rep. M.2413-0 (11/2017), 2017.

[35] Y. Wang, G. Leus, and A.-J. van der Veen, "Cramer-Rao bound for range estimation," in *Proc. IEEE Int. Conf. Acoust., Speech Signal Process.*, 2009, pp. 3301–3304.

Mostafa Mohammadkarimi (Member, IEEE) received the M.Sc. degree in electrical engineering from the K.N. Toosi University of Technology, Tehran, Iran, in 2011, and the Ph.D. degree from Memorial University, St. John's, NL, Canada, in 2017. From 2016 to 2017, he was a visiting Ph.D. Student with the Laboratory for Information and Decision Systems, Massachusetts Institute of Technology, Cambridge, MA, USA. From 2018 to 2021, he was a Postdoctoral Fellow with The University of Alberta, Edmonton, AB, Canada, The University of British Columbia, Vancouver, BC, Canada, and Friedrich-Alexander-Universität Erlangen-Nürnberg, Erlangen, Germany. Since 2021, he has been with the Signal Processing Systems Group, Department of Microelectronics, Delft University of Technology, Delft, The Netherlands. His research interests include wireless communications, statistical signal processing, AI for communications, and localization and navigation.

Geert Leus (Fellow, IEEE) received the M.Sc. and Ph.D. degrees in electrical engineering from KU Leuven, Leuven, Belgium, in 1996 and 2000, respectively. He is currently a Full Professor with the Faculty of Electrical Engineering, Mathematics and Computer Science, Delft University of Technology, Delft, The Netherlands. He was the recipient of the 2021 EURASIP Individual Technical Achievement Award, 2005 IEEE Signal Processing Society Best Paper Award, and 2002 IEEE Signal Processing Society Young Author Best Paper Award. He is a Fellow of EURASIP. He was a Member-at-Large of the Board of Governors of the IEEE Signal Processing Society, the Chair of the IEEE Signal Processing for Communications and Networking Technical Committee, Chair of the EURASIP Technical Area Committee on Signal Processing for Multisensor Systems, and Editor in Chief of the *EURASIP Journal on Advances in Signal Processing*. He is also the Editor in Chief of EURASIP Signal Processing.

Raj Thilak Rajan (Senior Member, IEEE) received the Ph.D. degree in electrical engineering from the Delft university of Technology, Delft, The Netherlands, in 2016. He is currently an Assistant Professor with the Faculty of Electrical Engineering, Mathematics and Computer Science, Delft University of Technology, and the Co-Director of the Delft Sensor AI Lab. He is an elected Member of the IAF SCAN (Space communications and Navigation) Committee, IEEE ASI (Autonomous Systems Initiative), and an Associate Editor for IEEE OPEN JOURNAL ON SIGNAL PROCESSING. His research interests include signal processing theory and methods for distributed autonomous sensing systems.